

Abradable Sealing Materials for Emerging IGCC-Based Turbine Systems

Kara J. Philips,¹ Maryam Zahiri Azar,¹ Timothy J. Montalbano,¹
Robert Vaßen² and Daniel R. Mumm¹

¹ Department of Chemical Engineering and Materials Science, University of California, Irvine

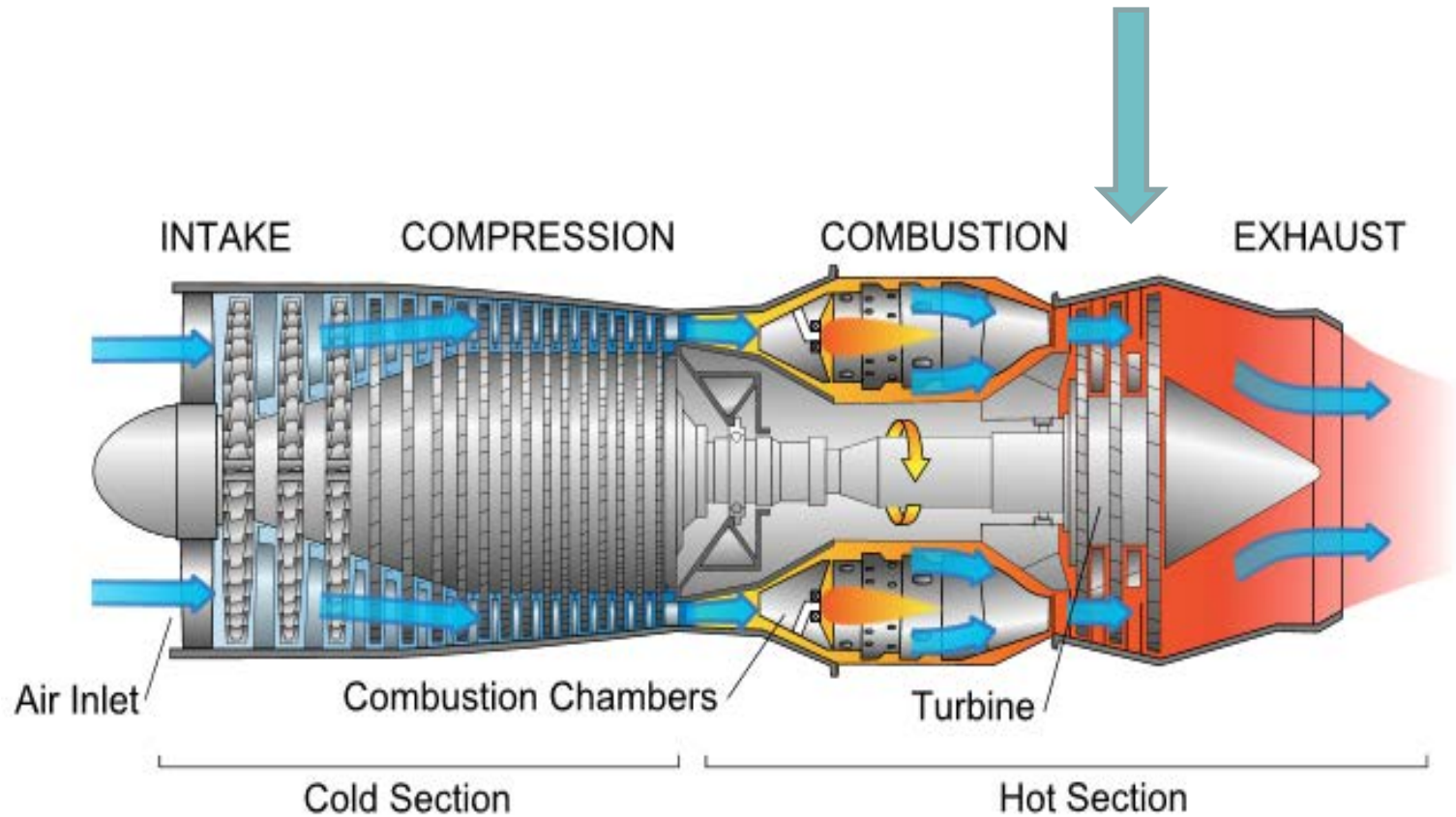
² IEK-1, Forschungszentrum Jülich, GmbH

2016 University Turbine Systems Research Workshop
Blacksburg, VA: November 2nd, 2016

DOE NETL Grant # DE-FE0011929
Project Manager: Dr. Robin Ames

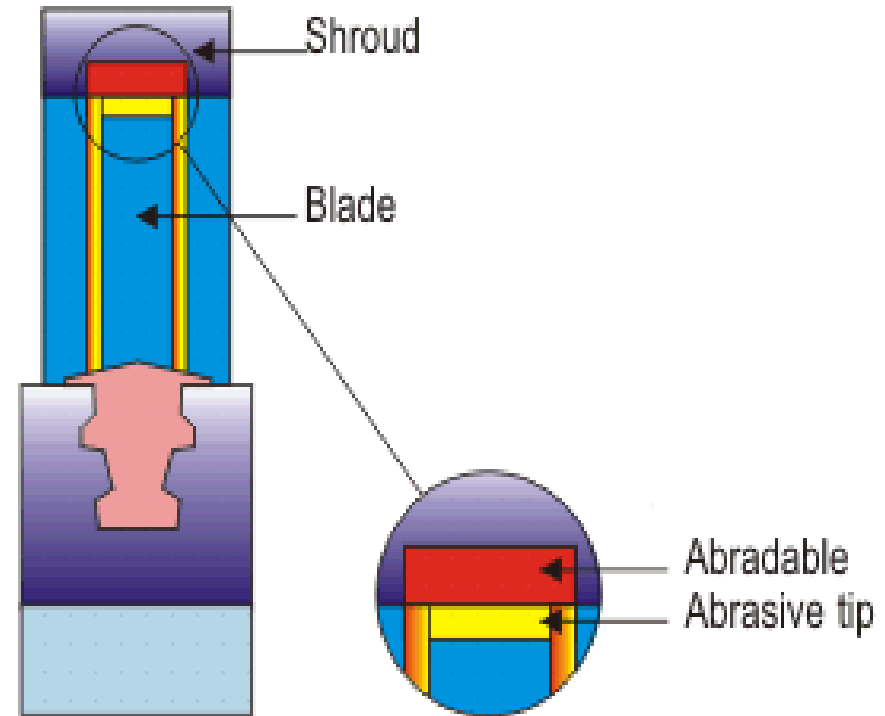
Clearance Control is Critical to Obtaining High Efficiency

Rotor-Shroud Clearance

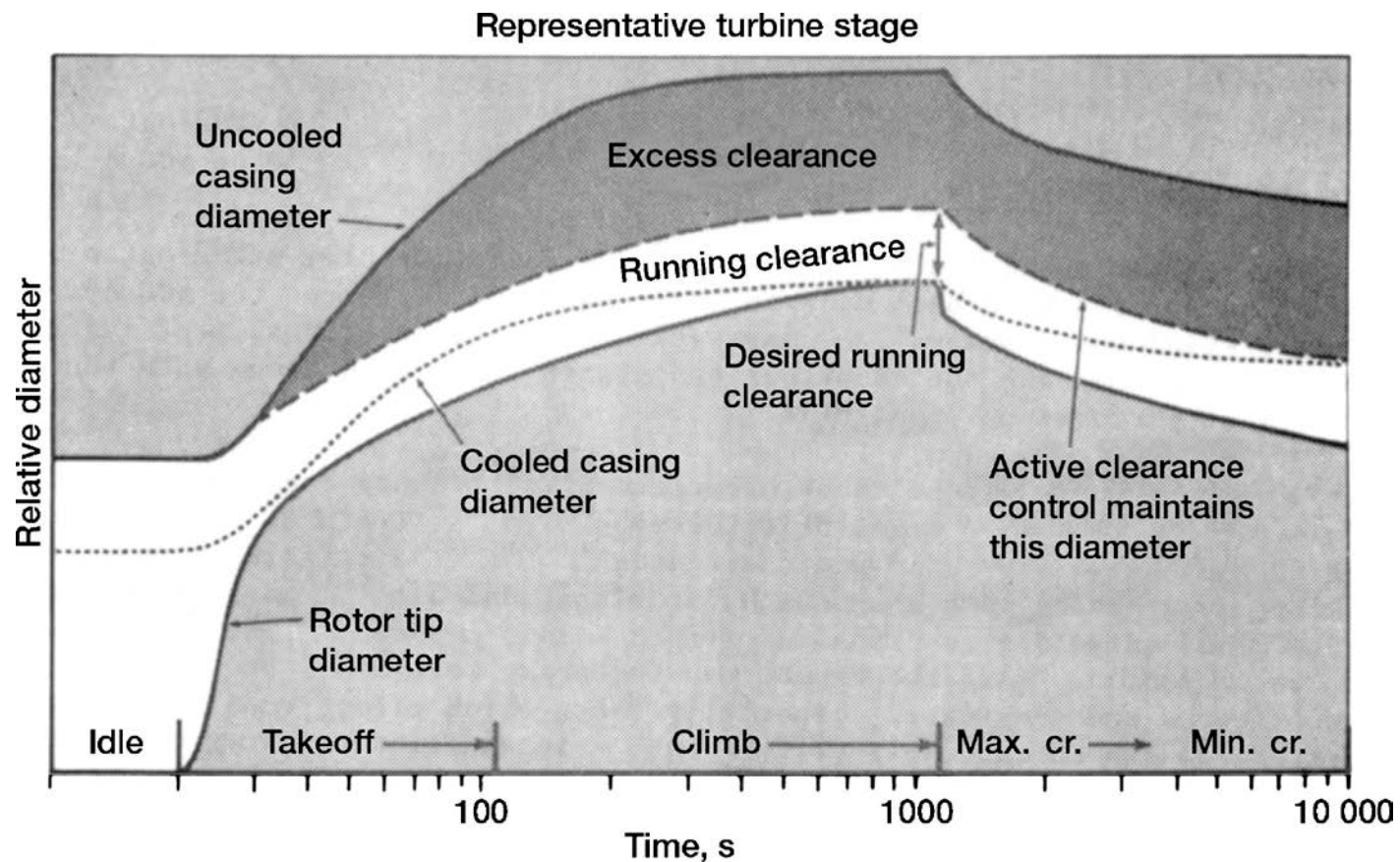


Abradable Materials for Clearance Control

- To reduce rotor-shroud clearance (an extra gap of .005" between the rotating blades and the engine casing can increase fuel consumption by as much as 0.5%).
 - Lower consumption of engine fuel
 - Improves engine-efficiency
- To achieve high temperature stability, low thermal conductivity, chemical stability, and erosion resistance at operating temperatures

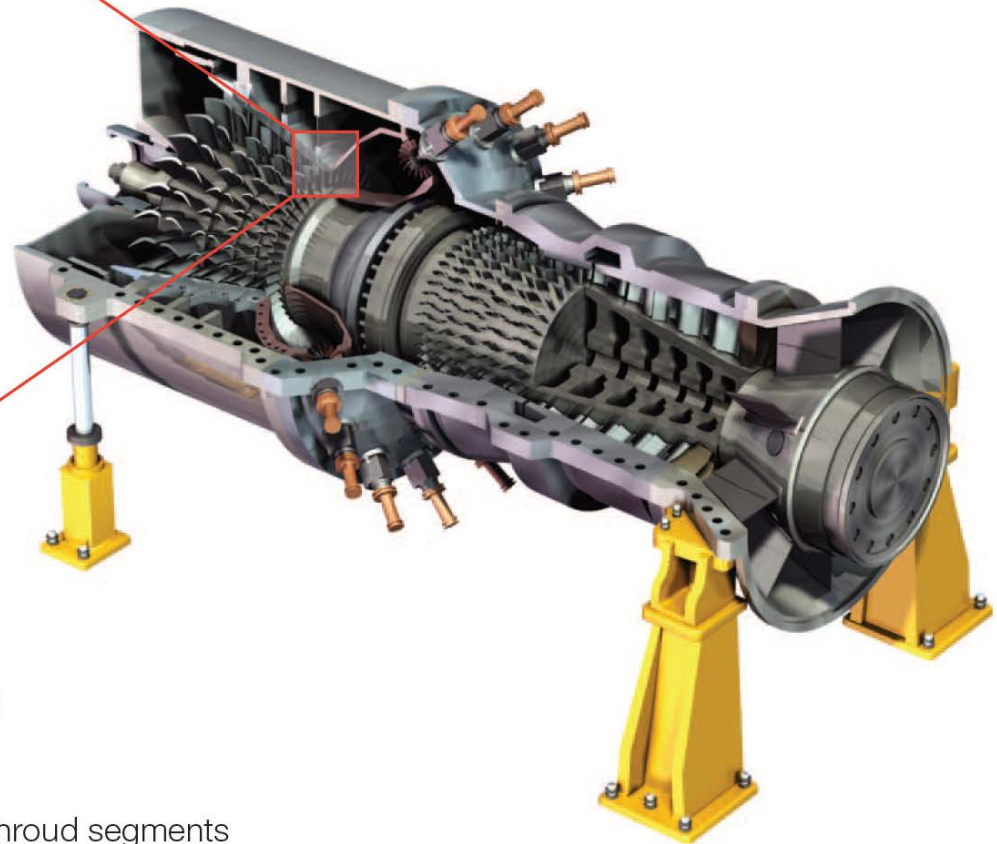
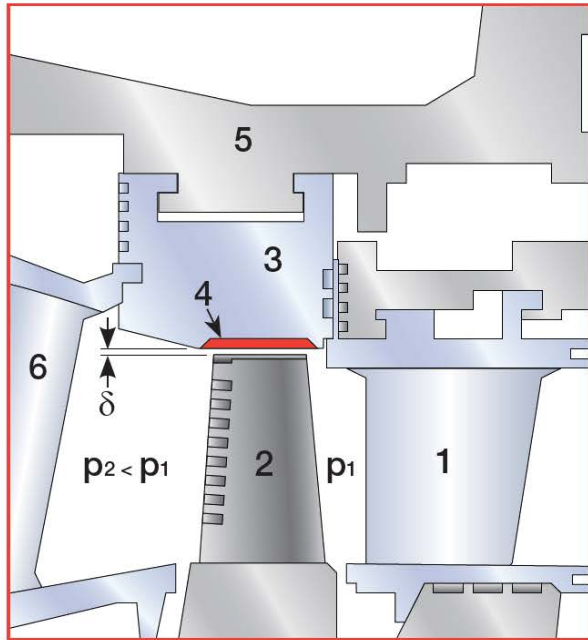


Active Cooling Control for Clearance Control



R.E. Chupp, et al., *Journal of Propulsion and Power*
Vol. 22, No. 2, March–April 2006

Abradable Seal Coatings

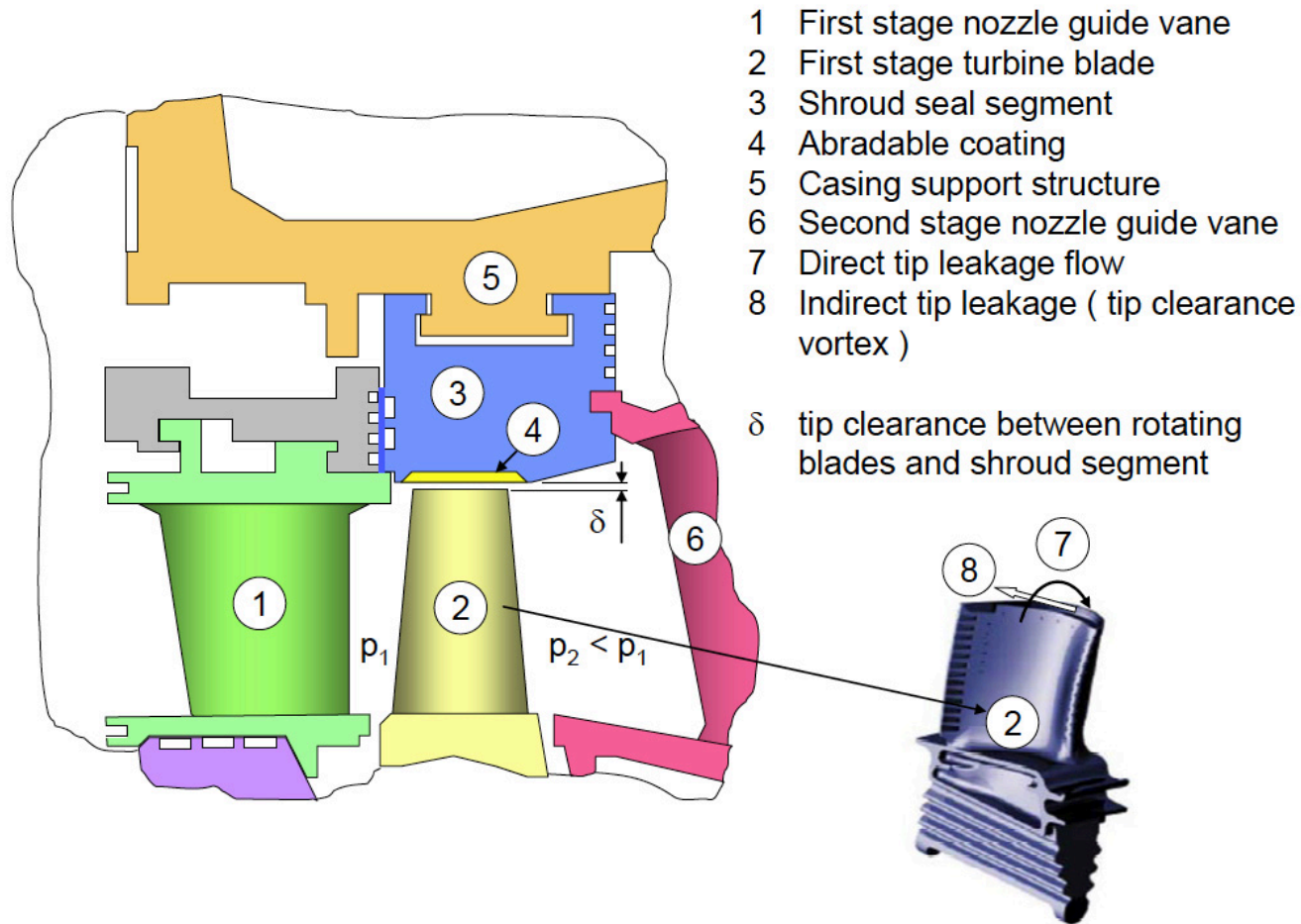


- 1 1st stage nozzle guide vane
- 2 1st stage turbine blade
- 3 shroud seal segment
- 4 high temperature ceramic abradable coating
- 5 casing support structure
- 6 2nd stage nozzle guide vane
- δ tip clearance between rotating blades and shroud segments

Sulzer Metco: SF-0015.0, July 2012

Abradable Seal Coatings

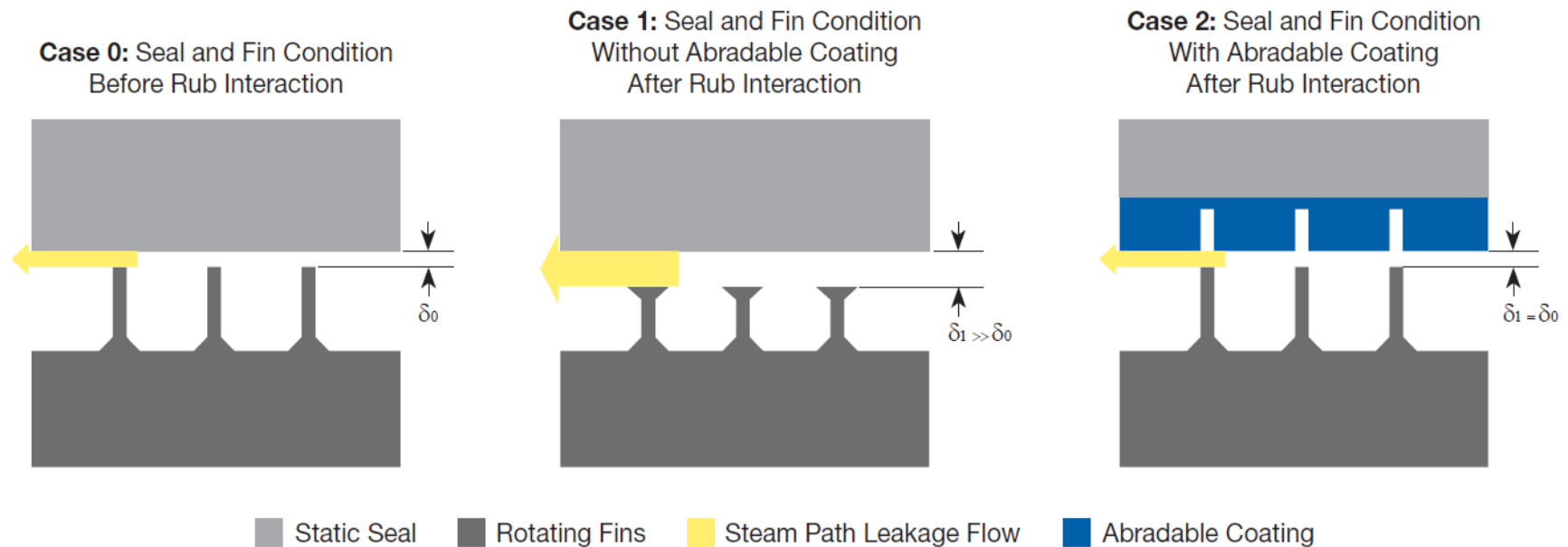
Schematic of a section through a gas turbine engine high pressure stage, showing where an abradable coating is used and how gas leaks through this seal leads to performance loss.



D. Sporer, S. Wilson and M. Dorfman, "Ceramics for Abradable Shroud Seal Applications." *Proceedings of the 33rd International Conference on Advanced Ceramics and Composites*, volume 3, 2009,

Potential Benefits of Abradables for Clearance Control

- Ideally, turbine/housing distance should be kept close to zero.
- Blade movement due to force and high heat would cause rubbing with housing
- Abradable designed to deform to form “trenches” where blades contact
- Theoretical efficiency increase of 1% or saves .39 trillion cubic feet of natural gas per year (calculated from IER estimate 2013)



Sulzer Metco, Solutions Flash Improve Efficiency and Reduce Emissions with Abradable Coatings for Steam Turbines, SF-0016.0, July 2012
<http://instituteeforenergyresearch.org/topics/encyclopedia/fossil-fuels/>

Abradable Materials

- Metal matrix ($T < 700$ degree C)
- Ceramic materials ($T > 700$ degree C)
- Lubricant/dislocator agent (hBN)
- Porous materials
- Ni/Graphite and AlSi/hBN for compressor
- CoNiCrAlY/hBN/Polyester for LP turbine sections of engines.
- YSZ, spinel or similar ceramics for HPT sections

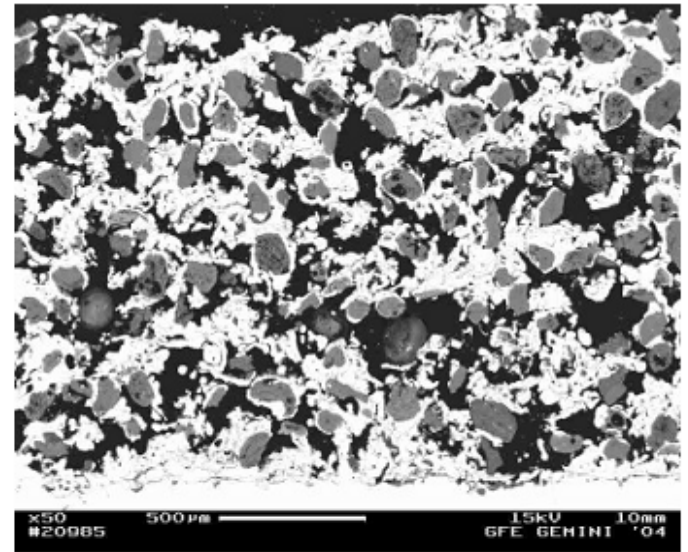
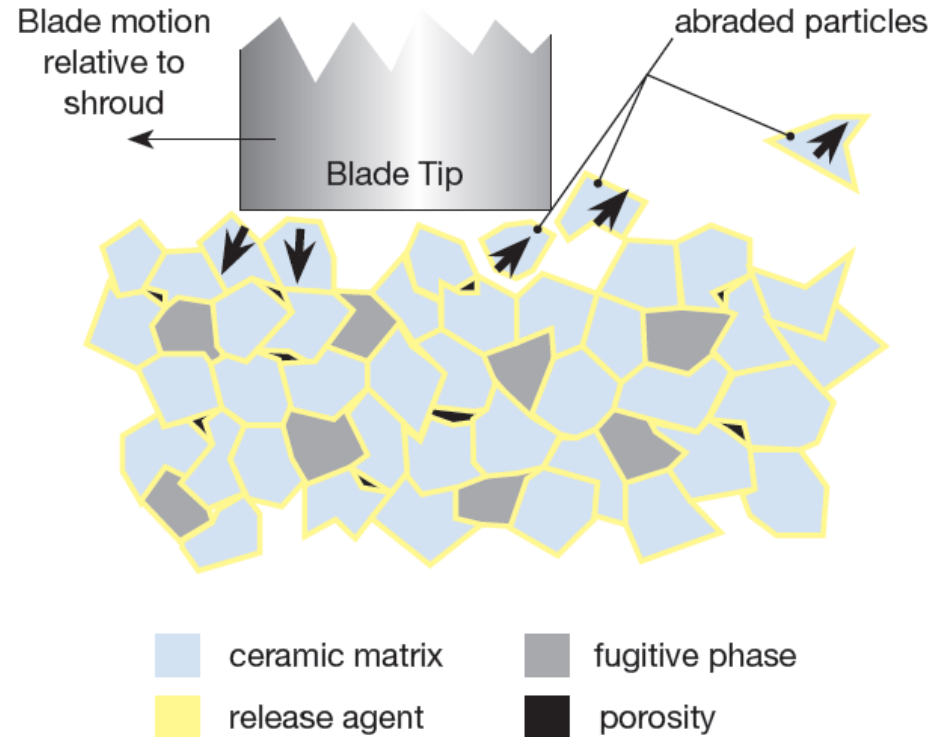


Figure 1: Cross section of a typical abrasion coating (dark phase: porosity, grey phase: bentonite, bright phase: NiCrAl metal matrix)

What is a Ceramic Abradable Coating?

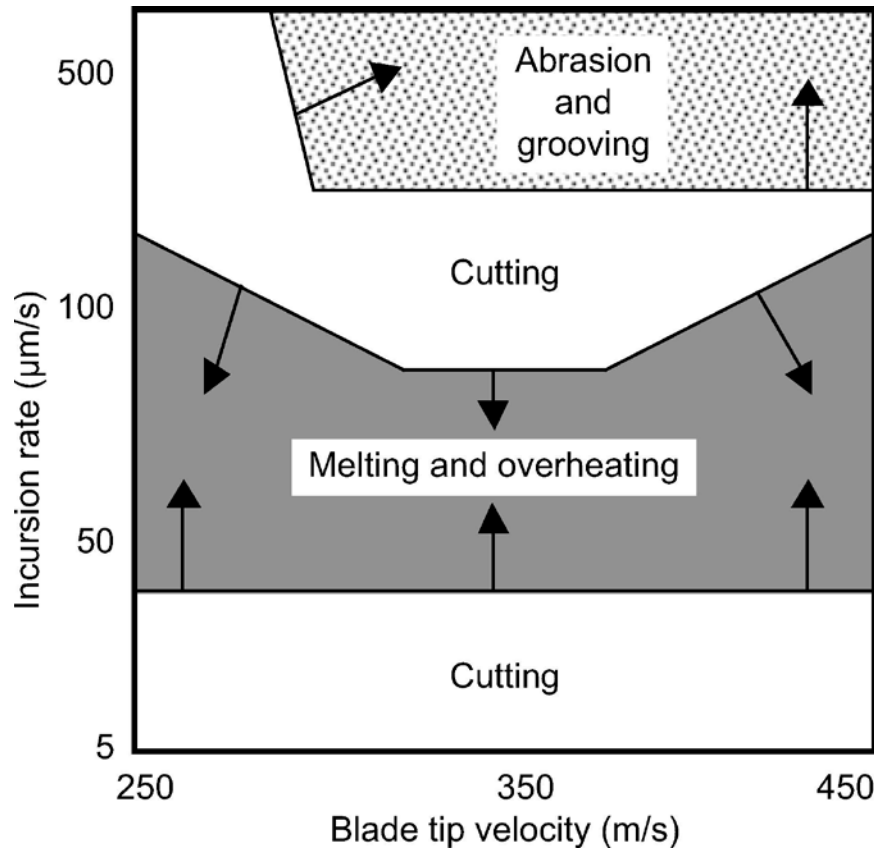
- Abradable coatings in turbines are generally made of a ceramic matrix with a fugitive phase and a release agent.
- Alternative release agent phases proposed are LaPO_4 and Spinel as a replacement for the whole system or in small concentration in YSZ.
- Mechanisms of mechanical degradation and microstructural evolution in corrosive and wet environments are not well documented.



Schematic representation of the abradable mechanism in service.

- Sulzer Metco, Solutions Flash Improve Efficiency and Reduce Emissions with Abradable Coatings for Steam Turbines, SF-0016.0, July 2012
- Ebert S, Mücke R, Mack D, Vaßen R, Stöver D, Wobst T, and Gebhard S, *J. Eur. Ceram Soc.* 33, (December 2013): 3335–43.
- Lyalin A, Nakayama A, Uosaki K, and Taketsugu T. *PCCP* 15, (January 31, 2013): 2809–20.

Abradability vs. Erosion – A Balancing Act (and Evolving)



Abradable Coating response is dependent upon operational parameters of the engine

R.E. Chupp, et al., *Journal of Propulsion and Power*, Vol. 22, No. 2, March–April 2006

- Concerns include: excessive blade-tip wear, macrorupture in coatings, transfer of materials from blade to shroud.

Abradability vs. Erosion – A Balancing Act (and Evolving)

- Housing coating must be ‘soft’ enough to wear away during startup.
- Must also be hard enough to not be eroded by debris

Too Soft



Heavy coating rupture
after initial blade
material transfer



Coating rupture

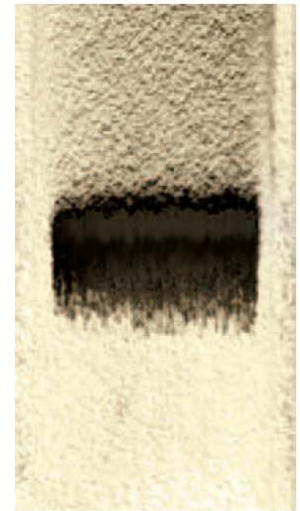


Slight coating rupture
mixed with cutting
and some blade
material transfer



Mixed coating rupture
and blade material
transfer

Too Hard



Heavy blade material
transfer

Sulzer Metco: SF-0015.0, July 2012

Ideal Wear Patterns – Tipped and Non-Tipped Blades

Ideal Wear Tracks

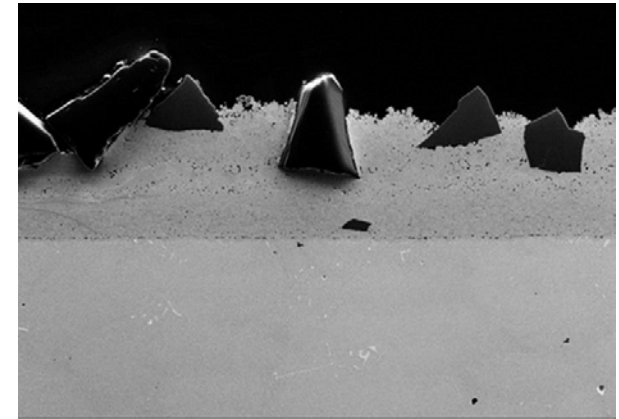
Un-tipped Blades



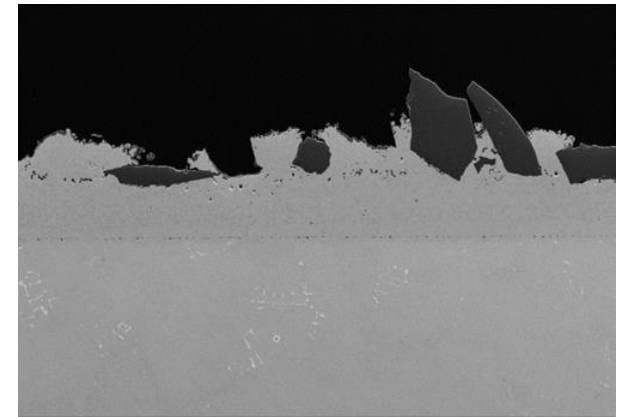
cBN-tipped
Blades



Sulzer Metco: SF-0015.0, July 2012



cBN Abrasive Coating: As-processed



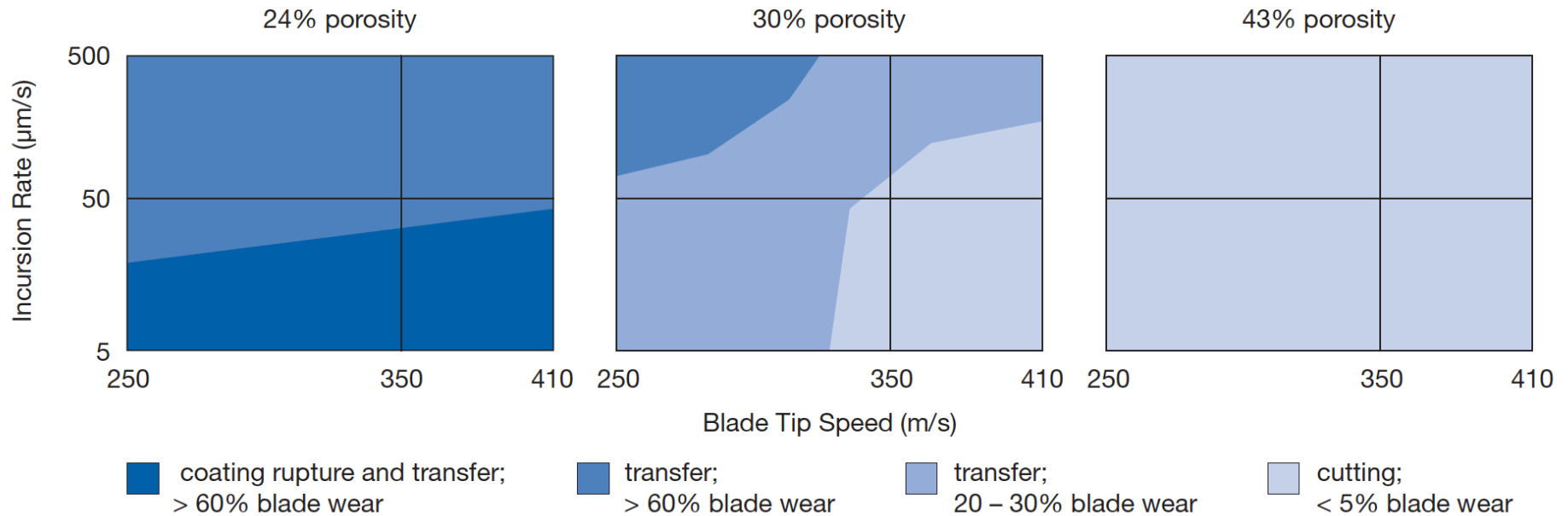
cBN Abrasive Coating: Oxidized

Scrinzi, E. et al. Development of New Abradable/Abrasive Sealing Systems for Clearance Control in Gas Turbines. ASME 2013 Proceedings.

The Role of Porosity on Abradability of Current Coatings

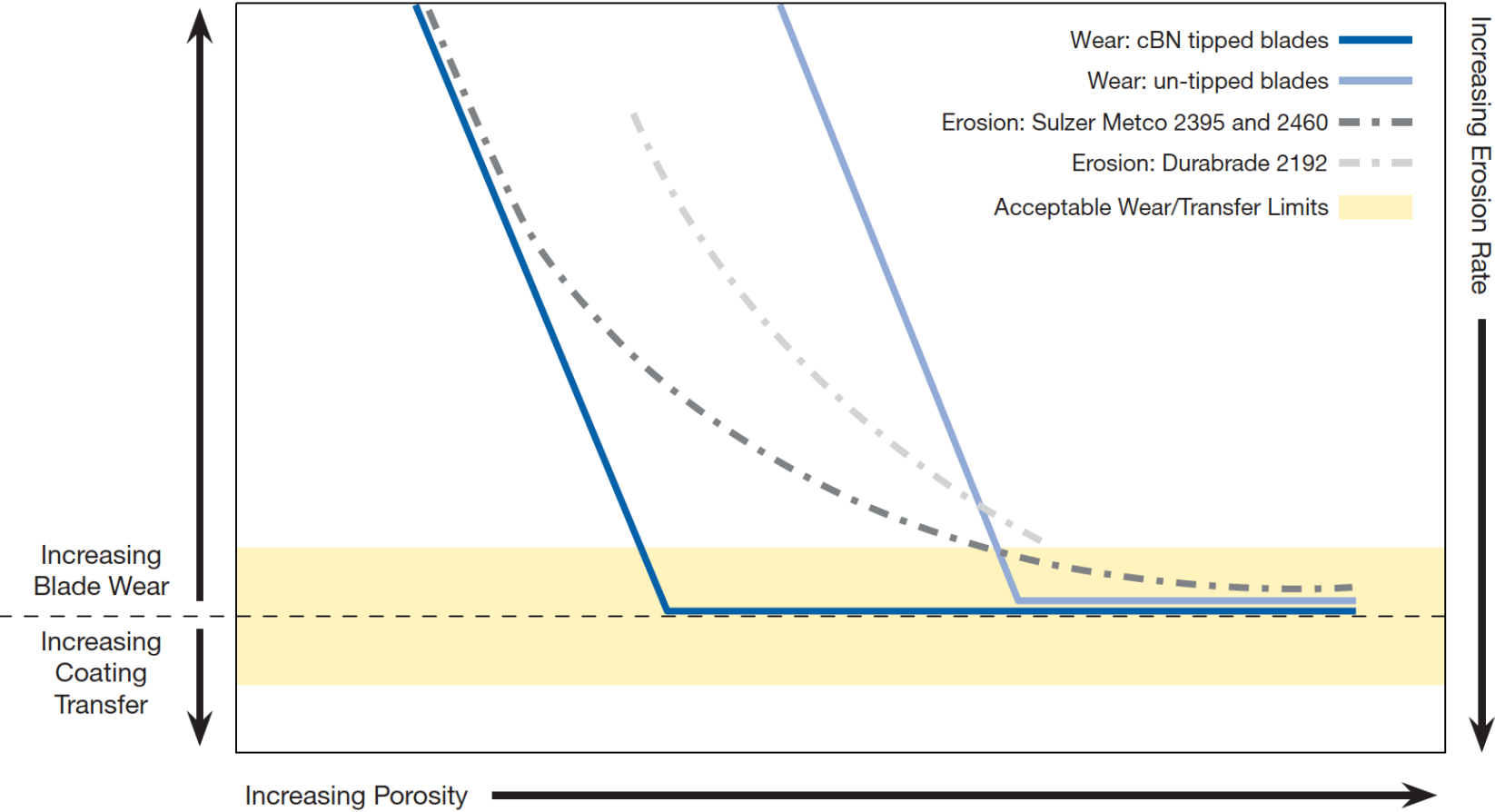
Porosity is optimized for reduced blade wear – but at the cost of erosion resistance.

Sample Abradable Wear Map Results at Varying Levels of Porosity Against Un-Tipped Blades



Sulzer Metco: SF-0015.0, July 2012

Abradability vs. Erosion – A Balancing Act (and Evolving)



Sulzer Metco: SF-0015.0, July 2012

Are prominent degradation modes for turbine hot-section materials exacerbated through the use of alternative fuels?

- ☑ High-Hydrogen Content (HHC) fuels may result in substantial increases in the water vapor content.
- ☑ Alternative fuels may introduce unique impurities that play a role in deposit-induced corrosion.

What are the mechanisms by which elevated water vapor contents may affect the durability and degradation of hot-section materials?

Project Overview

- Reducing the gap between rotating and stationary parts in gas turbine engines, and mitigating gas leakage via these paths, can significantly increase the performance and attendant efficiency. One approach to maintaining a minimum gap is to use abradable coatings on the stationary shroud components as seals.
 - Abradable coatings must be able to withstand high temperature oxidation, thermal cycling, and erosion, while providing optimal controlled abrasion and associated shape retention.
 - Syngas and high-hydrogen-content (HHC) fired turbines has shown that the stability of hot-section materials may be **substantially altered** due to characteristic changes in the combustion by-products (partial pressures of water vapor, etc.) as well as characteristic impurities and particulate matter entrained in the fuel.

Project Objectives

- ❑ Investigate the impacts of coal-derived syngas combustion environments on the performance, durability and degradation of existing abradable coatings used on turbine shroud structures.
- ❑ Assess the potential of alternative materials sets for improving performance of hot-section abradable seals **in IGCC-based gas turbine power plants.**
- ❑ Derive a **mechanisms-based understanding** of factors controlling the performance and degradation of abradable seals used in the high-temperature turbine sections of gas turbine engines in relation to emerging IGCC-based combustion environments, and evaluate the potential of alternative materials as abradable seal coatings – ultimately with the goal of developing a knowledge base upon which the design of coatings that retain optimal sealing characteristics and are more resistant to the observed wear/attack mechanisms.
- ❑ Educate the next generation of scientists and engineers trained in materials design for advanced turbine systems.

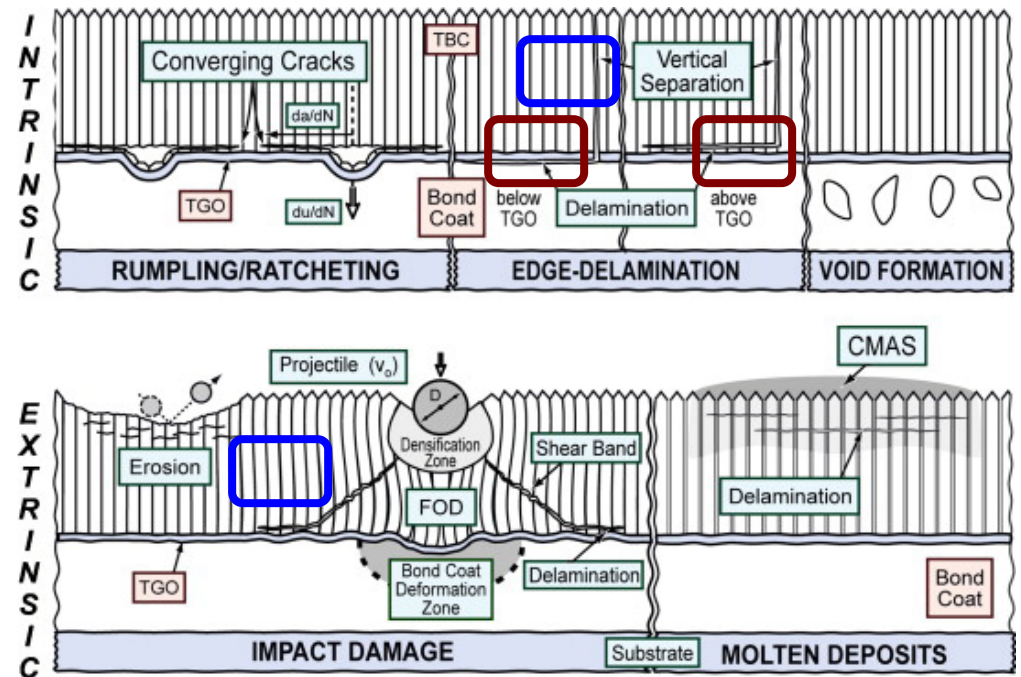
Outline

The research community has developed a mechanistic understanding of many (sometimes synergistic) prominent degradation modes. **How are these mechanisms influenced or modified by elevated water vapor content service conditions?**

Adapted from A.G. Evans (2007)

✓ Bond coat oxidation and TGO formation, and volatilization issues

✓ Phase evolution of the TBC top coat – loss of beneficial t' phase, and attendant monoclinic phase development

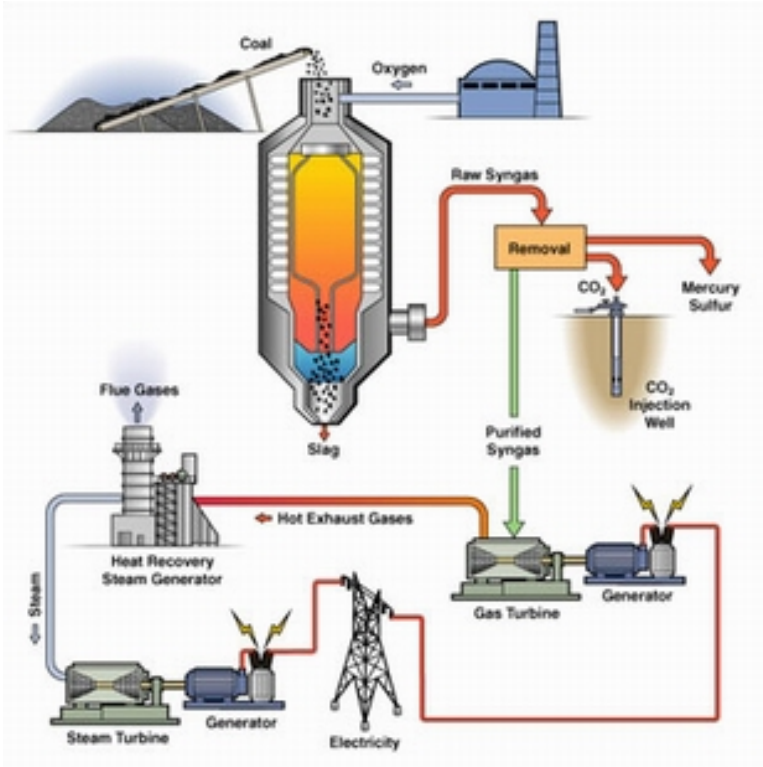


A.G. Evans, D.R. Clarke and C.G. Levi (2008)

Journal of the European Ceramic Society, 28, 1405-1419.

IGCC Process – High Hydrogen Content Fuels

Predicted Increased Water Content in Power Generation Turbines by the Use of Syngas



“Plug In, Charge Up, Drive Off” by Douglas L. Smith
 (calteches.library.caltech.edu/709/2/Drive.pdf)

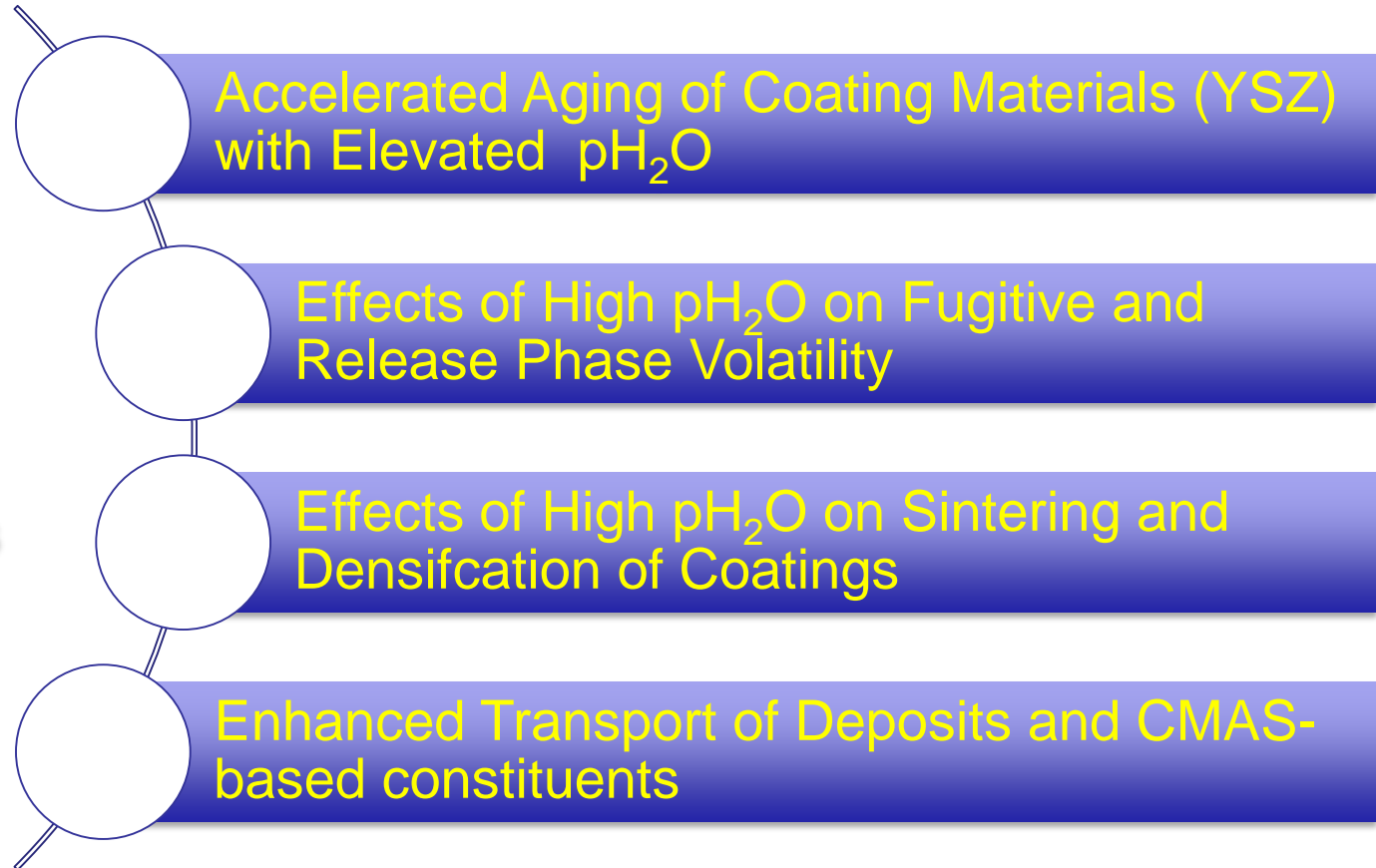
Flow Segment ID	Gas Composition				
	Units	GE Case 2	CoP Case 4	Shell Case 6	Range
Clean High-H ₂ Syngas	H ₂	91%	76%	86%	76-91%
	H ₂ O	0%	14%	3%	0-14%
	CO	2%	1%	3%	1-3%
	CO ₂	4%	2%	2%	2-4%
	Ar	1%	1%	1%	1%
Turbine Exhaust	N ₂	75%	74%	75%	74-75%
	H ₂ O	12%	14%	13%	12-14%
	O ₂	11%	10%	11%	10-11%
	CO ₂	1%	1%	1%	1%
	Ar	1%	1%	1%	1%

- **15-18 vol% H₂O** in turbine exhaust when using dry, high-H₂ syngas fuel
- If steam is used for NO_x suppression, H₂O could run as high as **30%**
- Represents a 2-4x increase over H₂O in natural gas combustion (**5-7%**)

White, Ames and Burke. National Energy Technology Laboratory (NETL) Report, 2013.

Spectrum of Possibilities for Accelerated Degradation

Implications of IGCC Combustion Environments

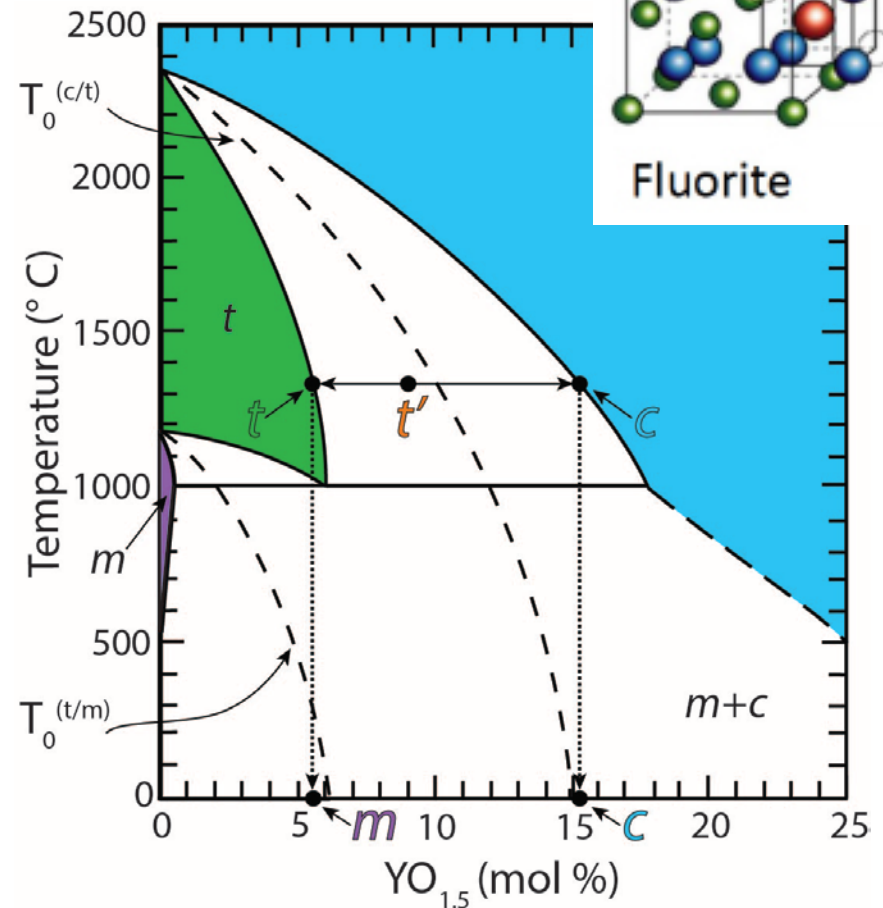


Accelerated Degradation in High pH₂O Environments

High Temp Aging of YSZ TBCs – Dependence on pH₂O ?

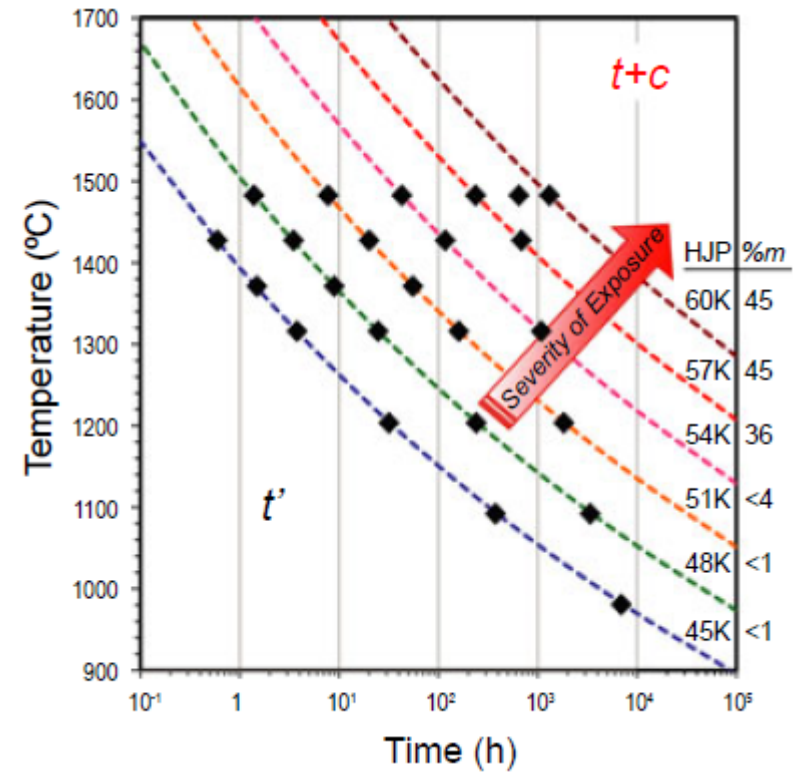
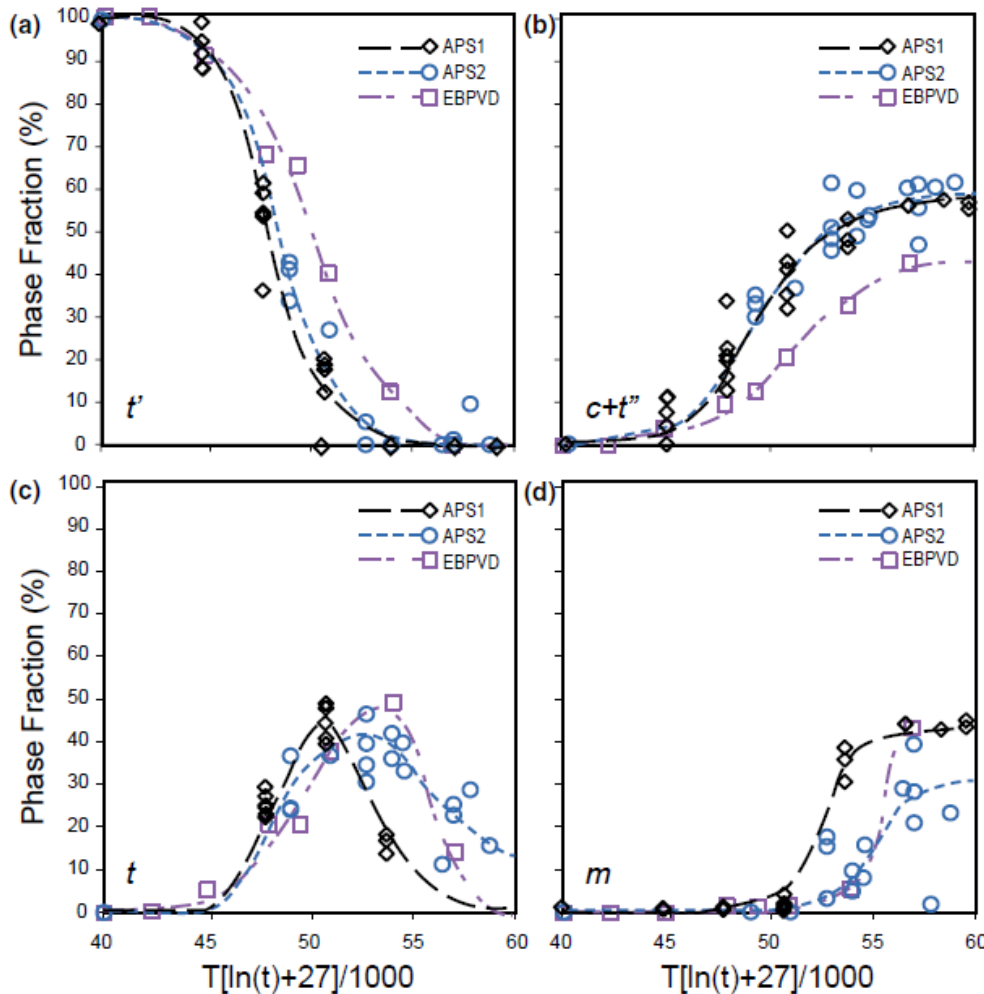
- Ytria content puts the 8YSZ in the tetragonal + cubic phase field
- t' phase will eventually decompose to the equilibrium tetragonal and cubic phases
- Rate is dictated by aging time and temperature
- Can normalize the influence of time and temperature by the use of the Larson-Miller or the Hollomon-Jaffe parameter of the form:

$$T[C + \ln(t)]$$



Redrawn from Levi *et al.*,
J. Am. Ceram. Soc., 96 [1] 290-298 (2013)

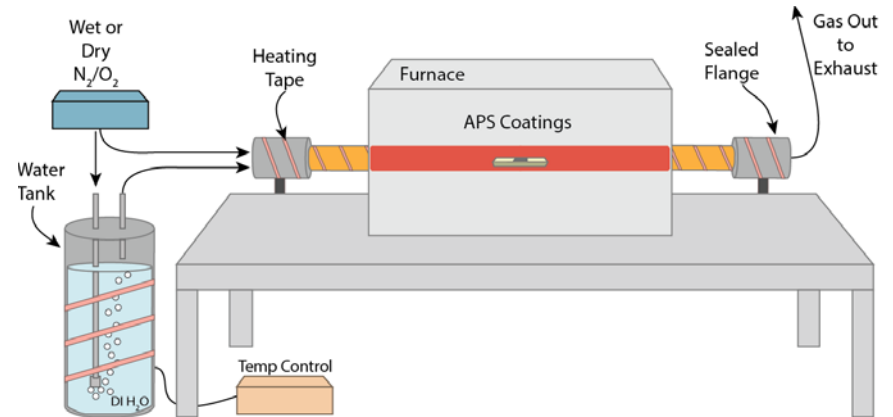
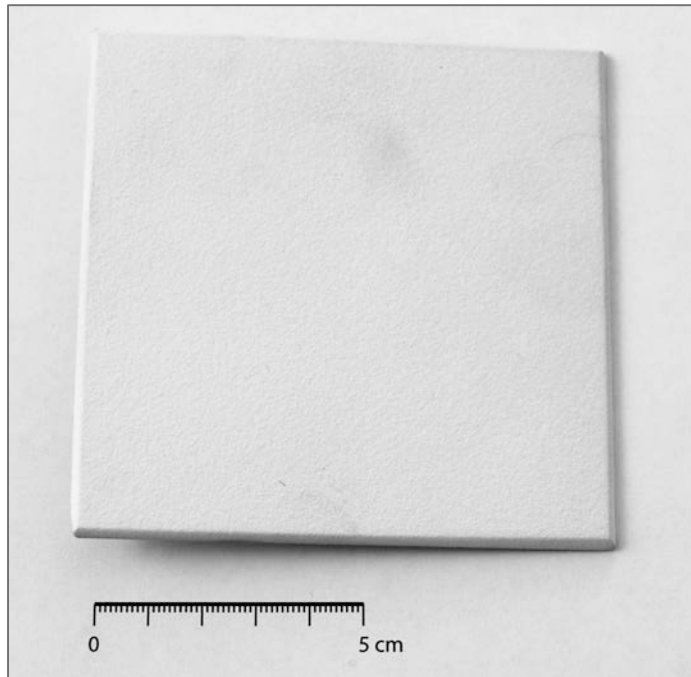
Prior Studies of Elevated Temp Aging of YSZ



Lipkin *et al.*, *J. Am. Ceram. Soc.*,
96 [1] 290-298 (2013)

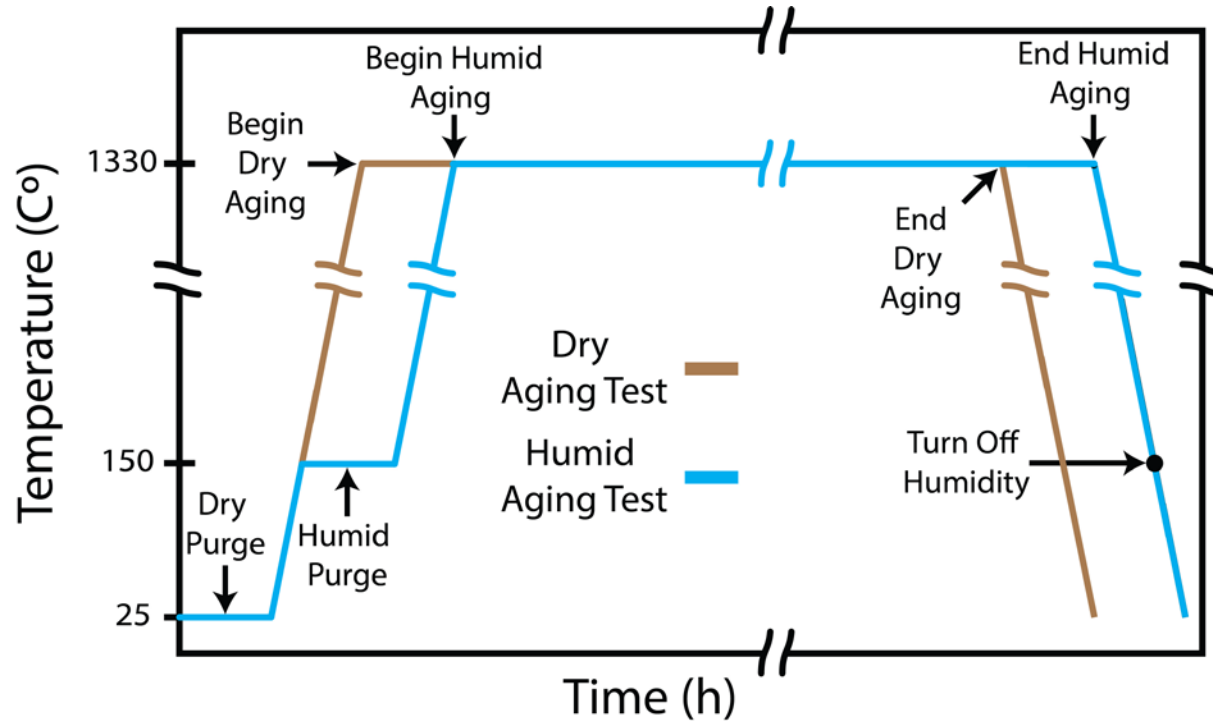
How does a humid environment influence the destabilization of the t' phase during aging?

Isothermal Aging Under Controlled pH₂O Conditions



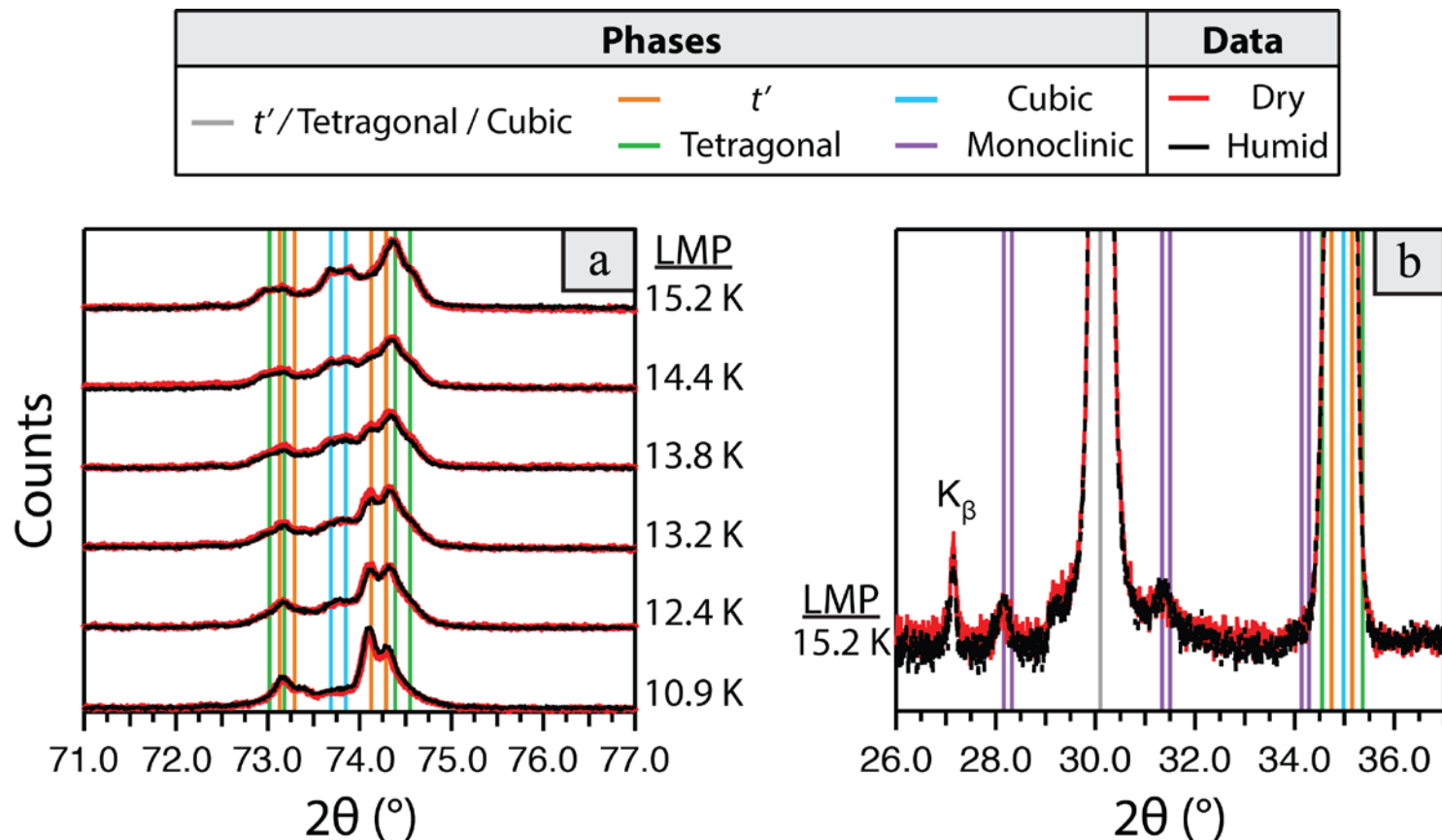
- Water tank temperature determines vol% H₂O via gas-liquid equilibrium exchange.
- For 0% H₂O, the water tank is bypassed completely.
- Exposed to dry or humid aging (30 vol%) in a controlled environment.
- Air plasma spray, 8 wt.% Yttria-Stabilized Zirconia.
- All test specimens cut from the same sample plate.

Aging Protocols and Materials Characterization



- Post-test characterization by XRD, Raman, XPS and microstructural analysis via TEM/STEM imaging.
- Rietveld refinement of XRD spectra to quantify evolving phase fractions. The refinement employed a four phase model (t' , tetragonal, cubic and monoclinic)

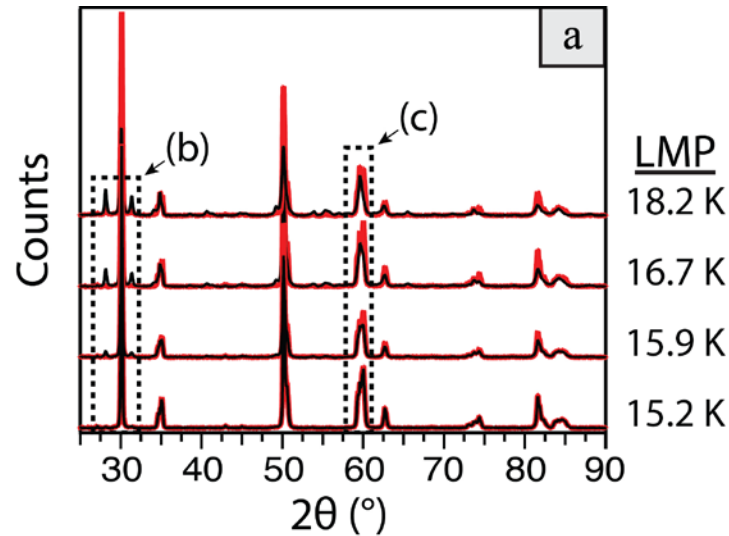
XRD Analysis of Aging to LMP = 15.2k (88 hours exposure)



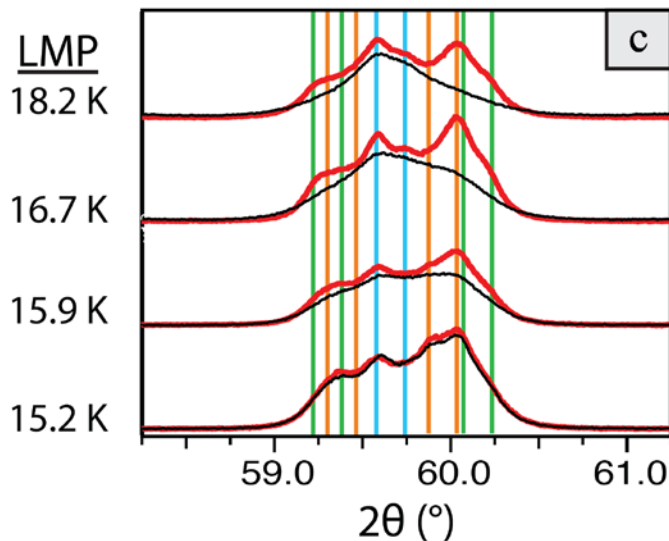
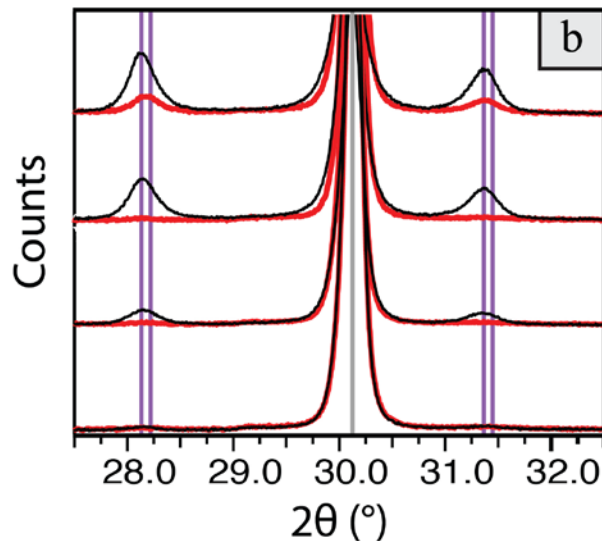
- XRD peak positions gradually shift from t' toward tetragonal and cubic positions.
- Indicates a range of lattice parameters as the t' is destabilized.
- No significant difference observed between 'dry' and 'humid' conditions.

Further Aging to LMP = 18.2k (570 hours exposure)

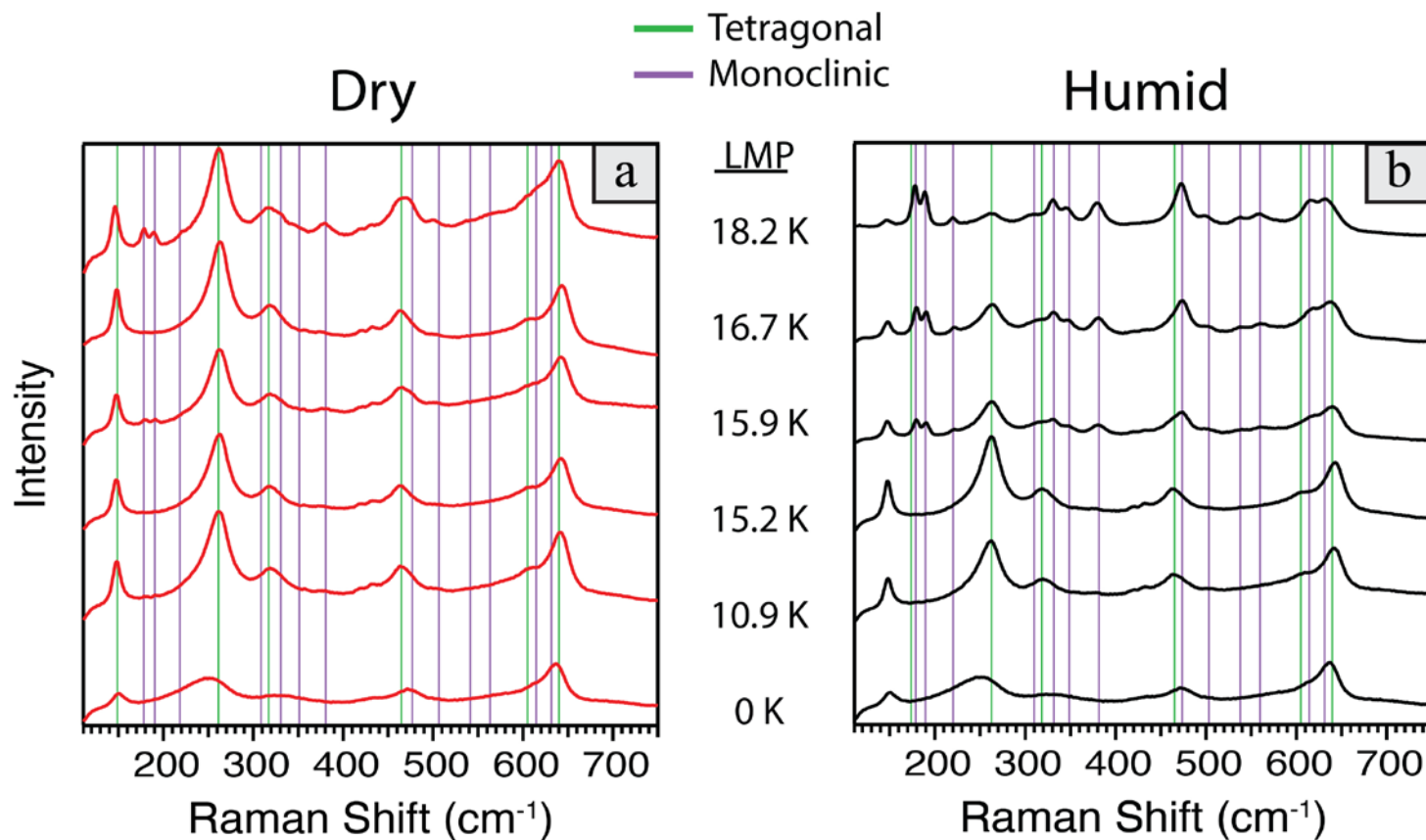
Data	
—	Dry
—	Humid
Phases	
—	t'
—	Tetragonal
—	Cubic
—	Monoclinic
—	$\left(\begin{array}{c} t' \\ \text{Tetragonal} \\ \text{Cubic} \end{array} \right)$



Accelerated formation of the monoclinic phase observed under elevated pH_2O conditions



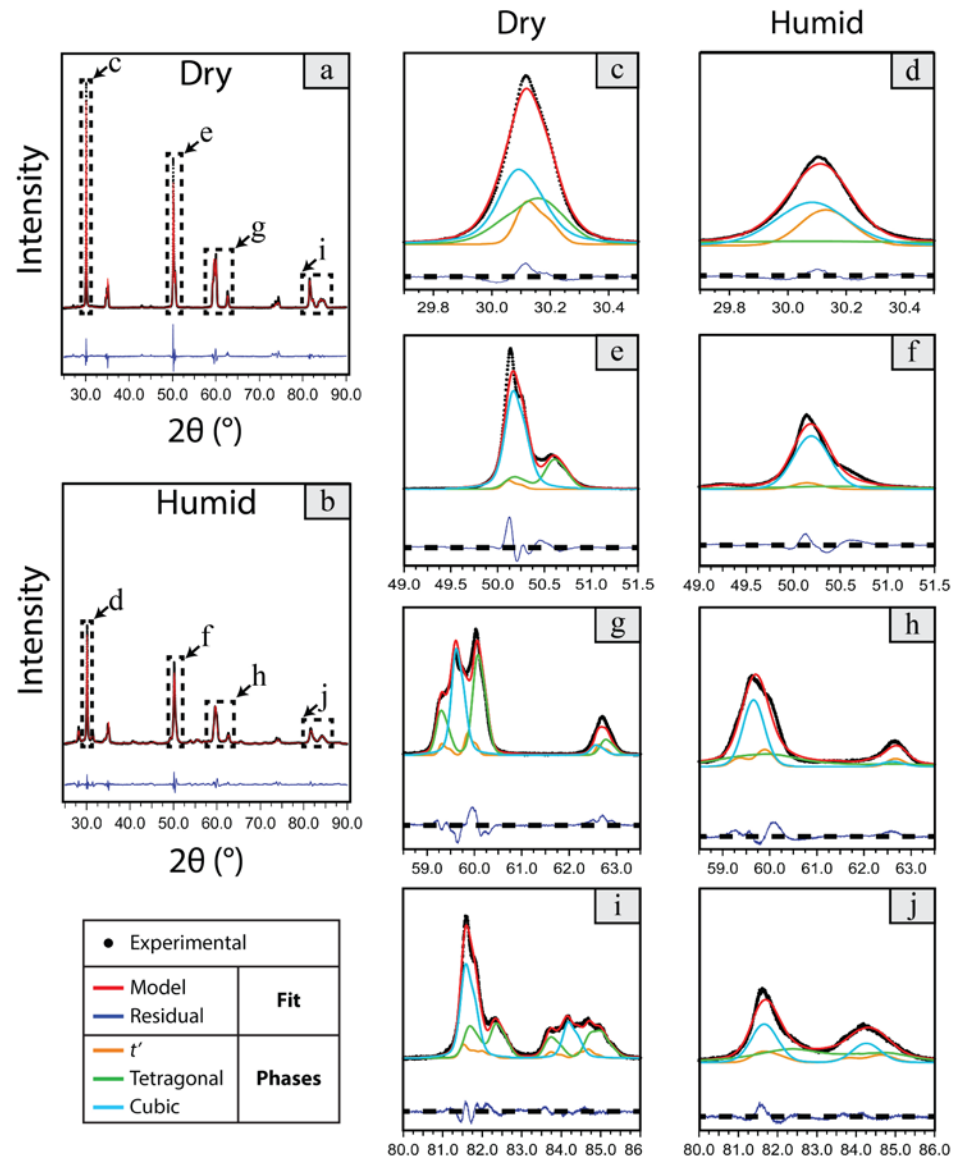
Raman Spectroscopy Analysis Corroborates XRD Results



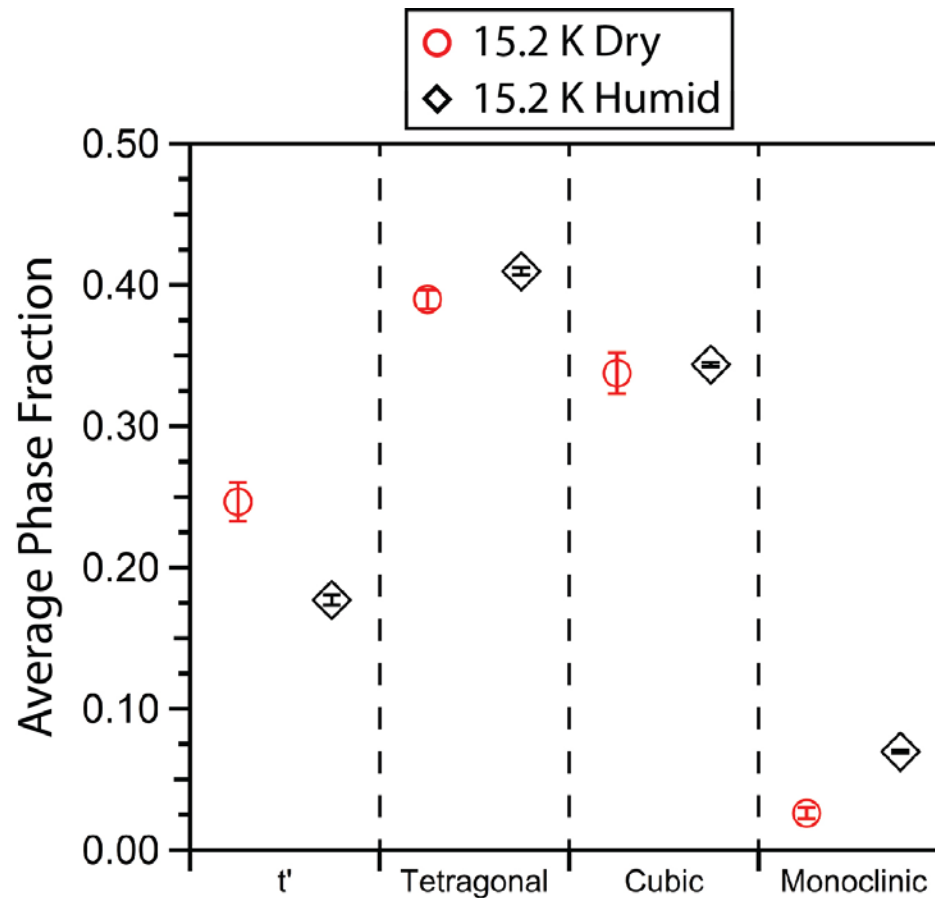
- For dry aging, the monoclinic modes not observed until LMP = 18.2 K (570 h)
- For humid aging, the monoclinic modes appear as soon as 15.9 K (140 h)

Quantitative Phase Fraction Analysis of XRD Results

- Full-pattern Rietveld fitting
- Examples of the peak deconvolution shown
- Selected peaks corresponding to the t' , tetragonal and cubic phases
- Weighted profile R value (a metric for quality of fit) was consistently less than 7%

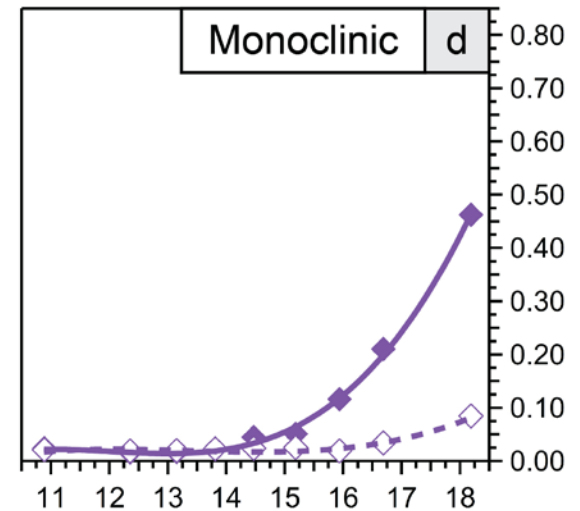
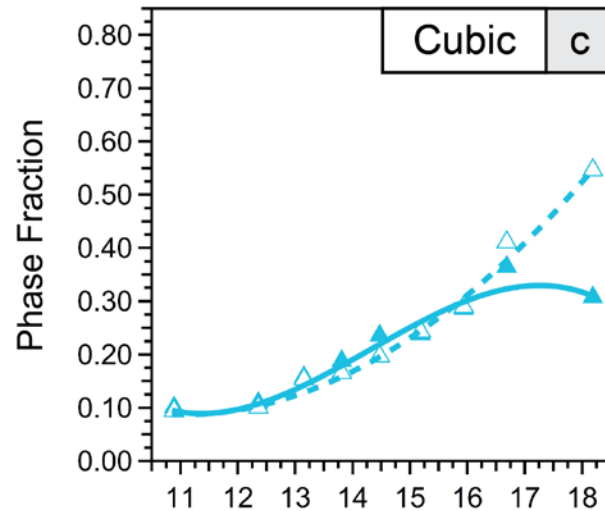
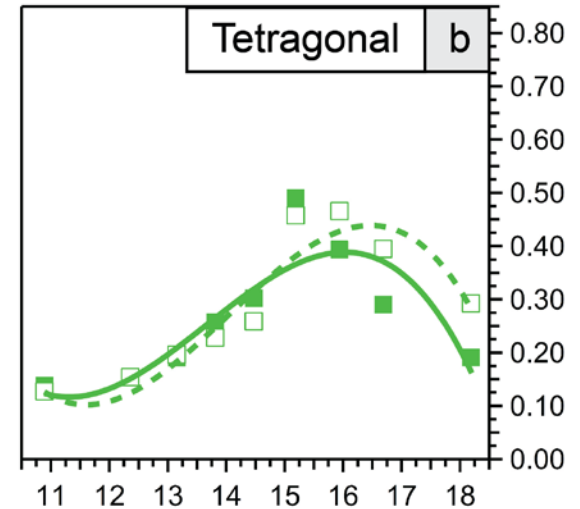
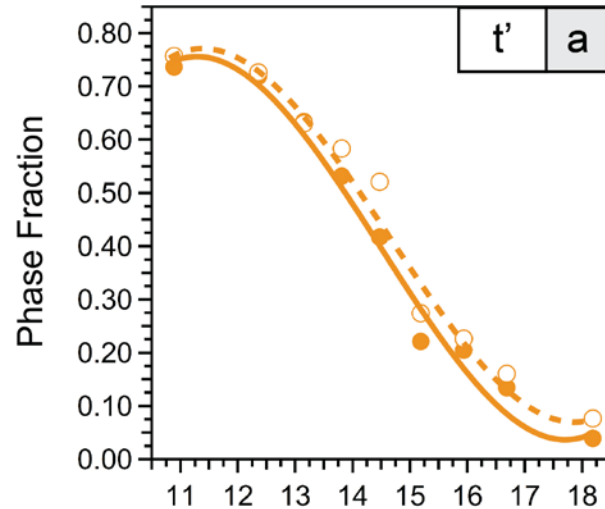


Average Phase Fractions at LMP = 15.2k (88 hours exposure)



- Accelerated decomposition of the t' phase, with associated formation of the monoclinic phase.

Evolution of the Phase Fractions with Exposure Time

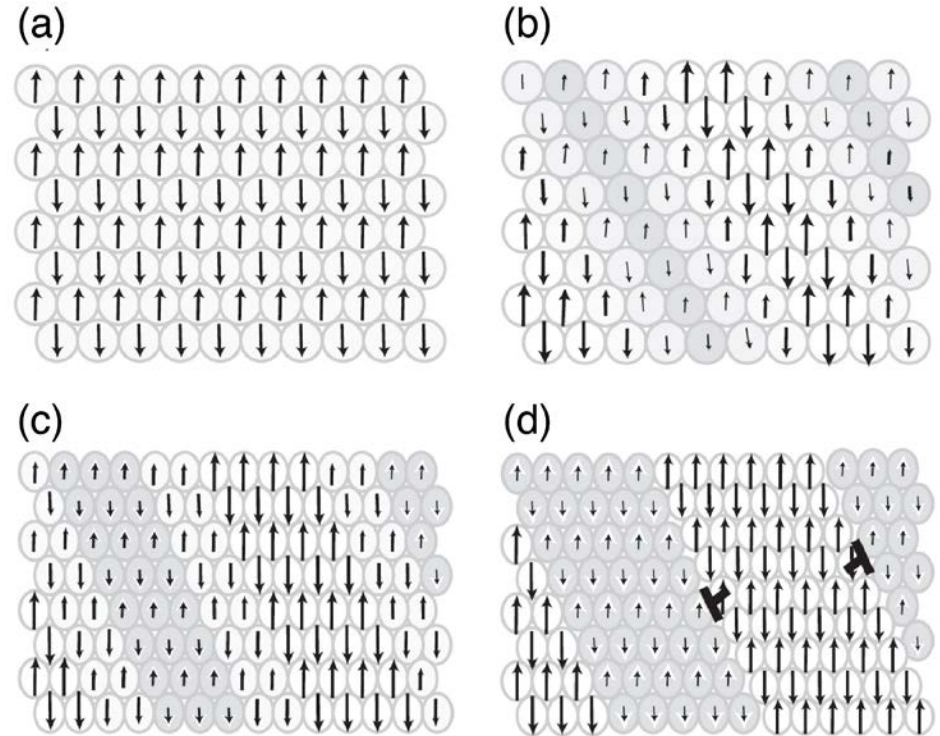


Larson-Miller Parameter ($\cdot 10^{-3}$)

Larson-Miller Parameter ($\cdot 10^{-3}$)

Evolution of the Phase Fractions with Exposure Time

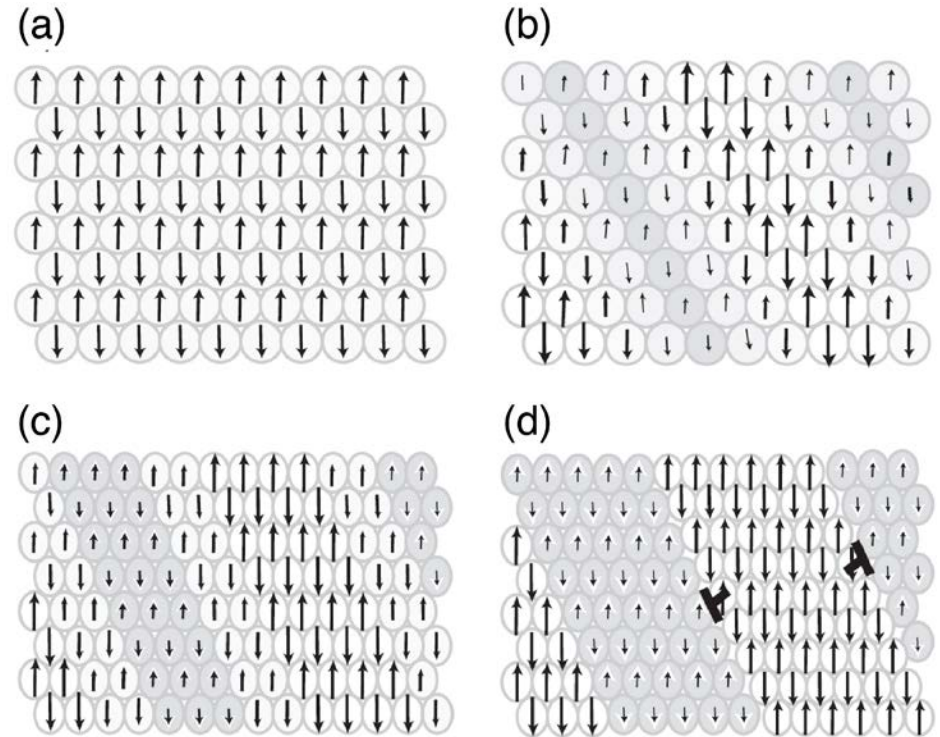
- ✧ In early stages of evolution, coherency strains prevent Y-rich and Y-lean phases from relaxing to equilibrium lattice structures; system appears as single-phase t'
- ✧ Interfacial coherency provides a driving force for coarsening; a wide variation in tetragonality develops with an associated variation in lattice parameters



Krogstad *et al.*, *J. Am. Ceram. Soc.*, 94 [S1] S168-S177 (2011)

Evolution of the Phase Fractions with Exposure Time

- ✧ Continued coarsening results in larger fractions of the system relaxing to equilibrium lattice parameters, and a sharpening of the strain gradient at domain boundaries
- ✧ Misfit dislocations are introduced to relieve coherency strains, allowing further development of the Y-lean (tetragonal) and Y-rich (cubic) phases. The Y-lean domains are now transformable to monoclinic



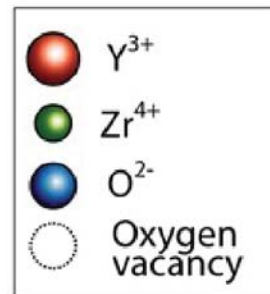
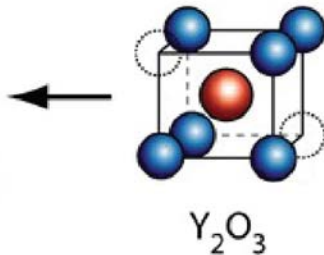
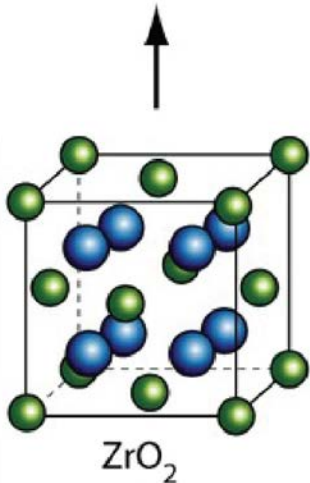
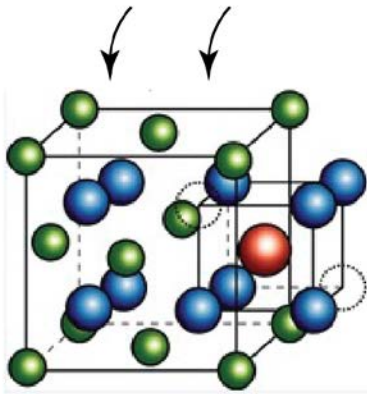
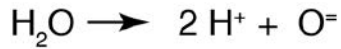
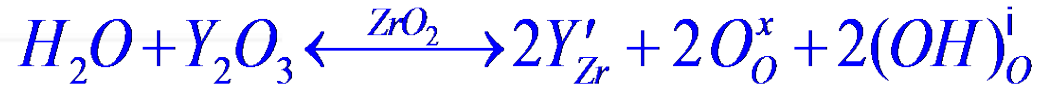
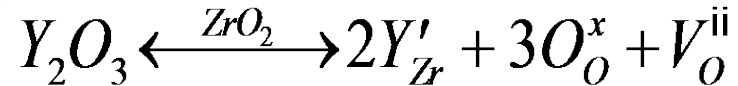
Krogstad *et al.*, *J. Am. Ceram. Soc.*, 94 [S1] S168-S177 (2011)

Potential Mechanism for pH₂O Dependence

Clarke et al., *J. Am. Ceram. Soc.*, 92 [9] 1901-1920 (2009)



Prinz et al., *Chem. Mater.*, 22 5366-5370 (2010)



Dissociation of water, and incorporation of protons and oxygen ions, may be accommodated through changes in the defect chemistry.

Rate Controlling Defects & Potential Interactions w/ Water Species



Philosophical Magazine A



ISSN: 0141-8610 (Print) 1460-6992 (Online) Journal homepage: <http://www.tandfonline.com/loi/tpa20>

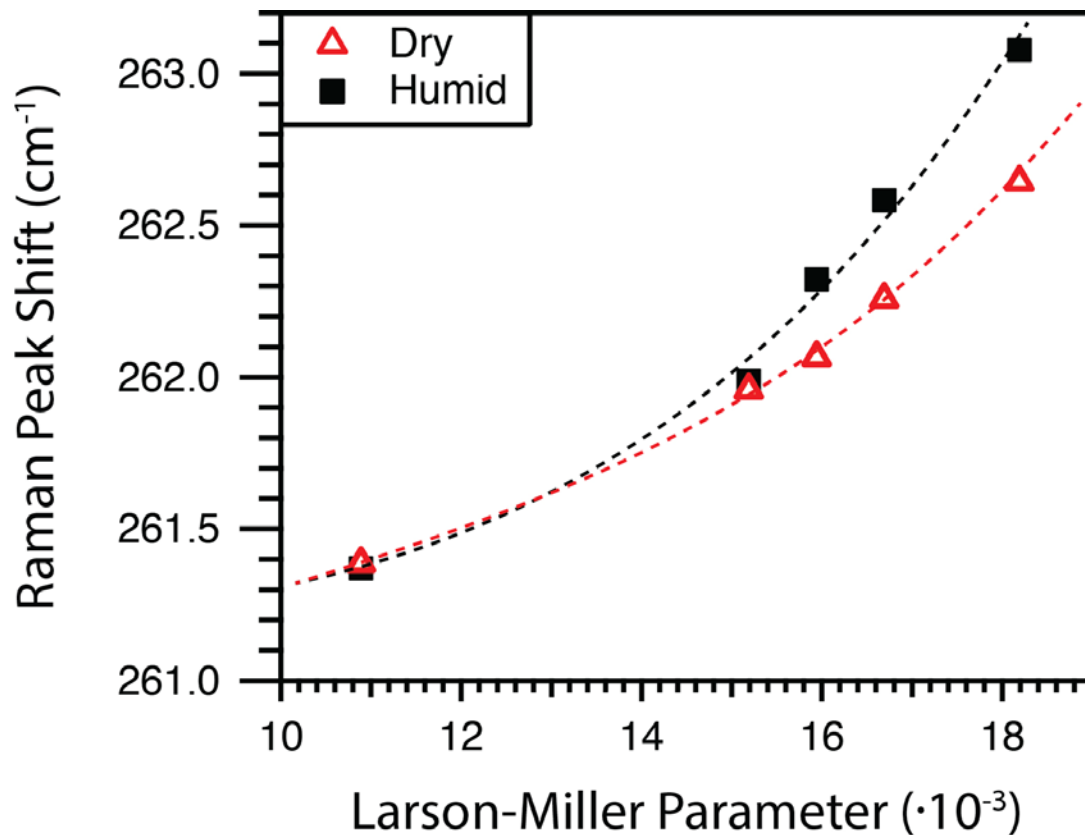
Lattice diffusion kinetics in Y_2O_3 -stabilized cubic ZrO_2 single crystals: A dislocation loop annealing study

F. R. Chien & A. H. Heuer

To cite this article: F. R. Chien & A. H. Heuer (1996) Lattice diffusion kinetics in Y_2O_3 -stabilized cubic ZrO_2 single crystals: A dislocation loop annealing study, Philosophical Magazine A, 73:3, 681-697, DOI: [10.1080/01418619608242990](https://doi.org/10.1080/01418619608242990)

- Studied cation diffusion through measurements of shrinkage rates of prismatic dislocation loops introduced through plastic deformation.
- Noted that cation diffusion in 18 mol% YSZ is 15 times slower than in 9.4 mol% YSZ; however, activation energies for both materials nearly identical.
- Studies suggested that a charged vacancy cluster, the divacancy: $(V_O^{ii} V_{Zr}^{iii})''$ is rate controlling.
- Furthermore, the lower cation diffusivities of the higher-solute compositions are attributed to the higher density of yttrium-containing trapping and blocking centers: $(Y'_{Zr} V_O^{ii})'$ and Y'_{Zr} respectively.

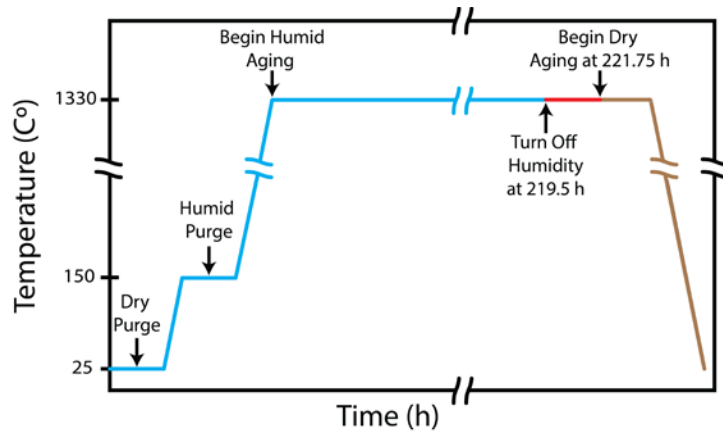
Raman Consistent w/ Relaxing of Interface Coherency Strain



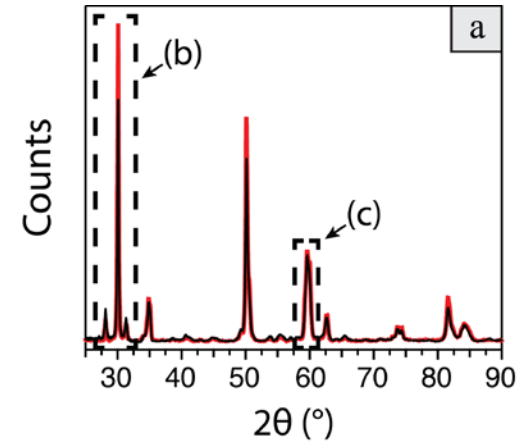
Peak fitting of the A_{1g} mode shows peak shifting in both environments

- Indicates a continuous change in the lattice parameters
- Peak shifts faster for humid-aging condition

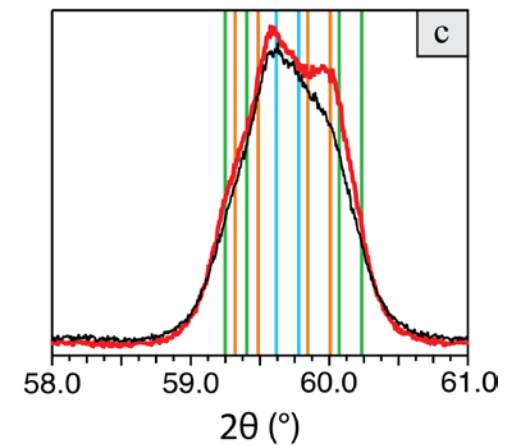
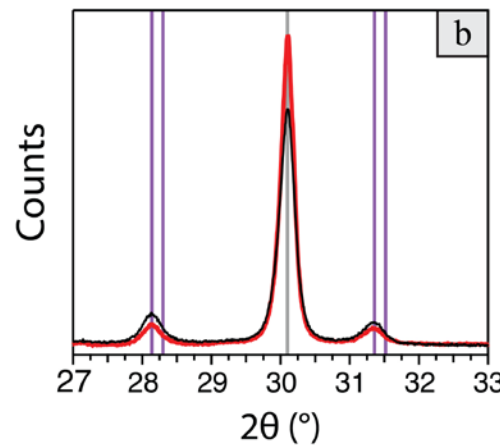
Confirmation of High Temp Effect (not LTD Artifact)



Data	
—	Dry
—	Humid
Phases	
—	t'
—	Tetragonal
—	Cubic
—	Monoclinic
—	(t')
—	(Tetragonal)
—	(Cubic)

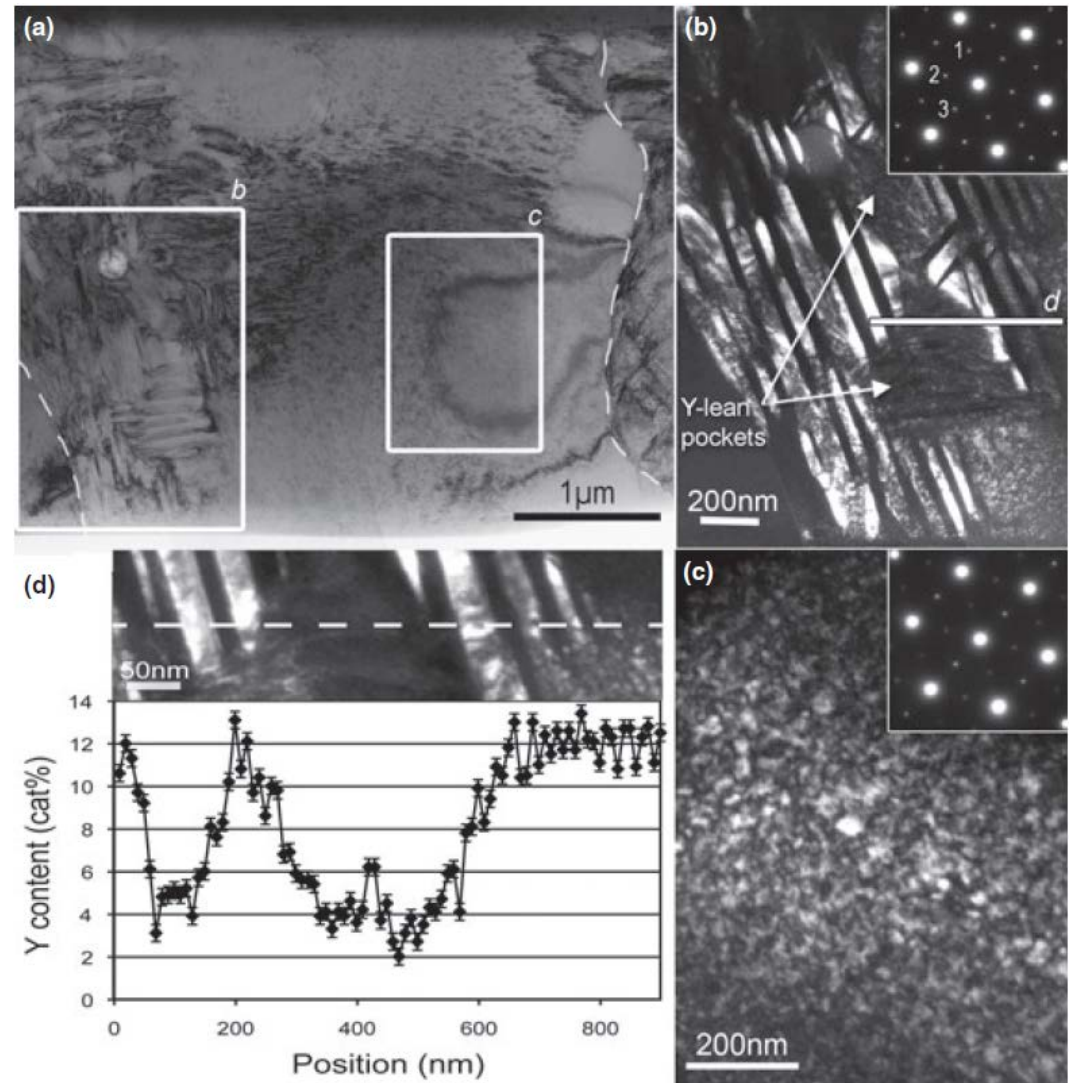


Observed monoclinic formation appears to play out at high temperature, not as an artifact of low temperature exposure to high p_{H₂O} conditions.



Structural Verification of Accelerated Coarsening/Aging

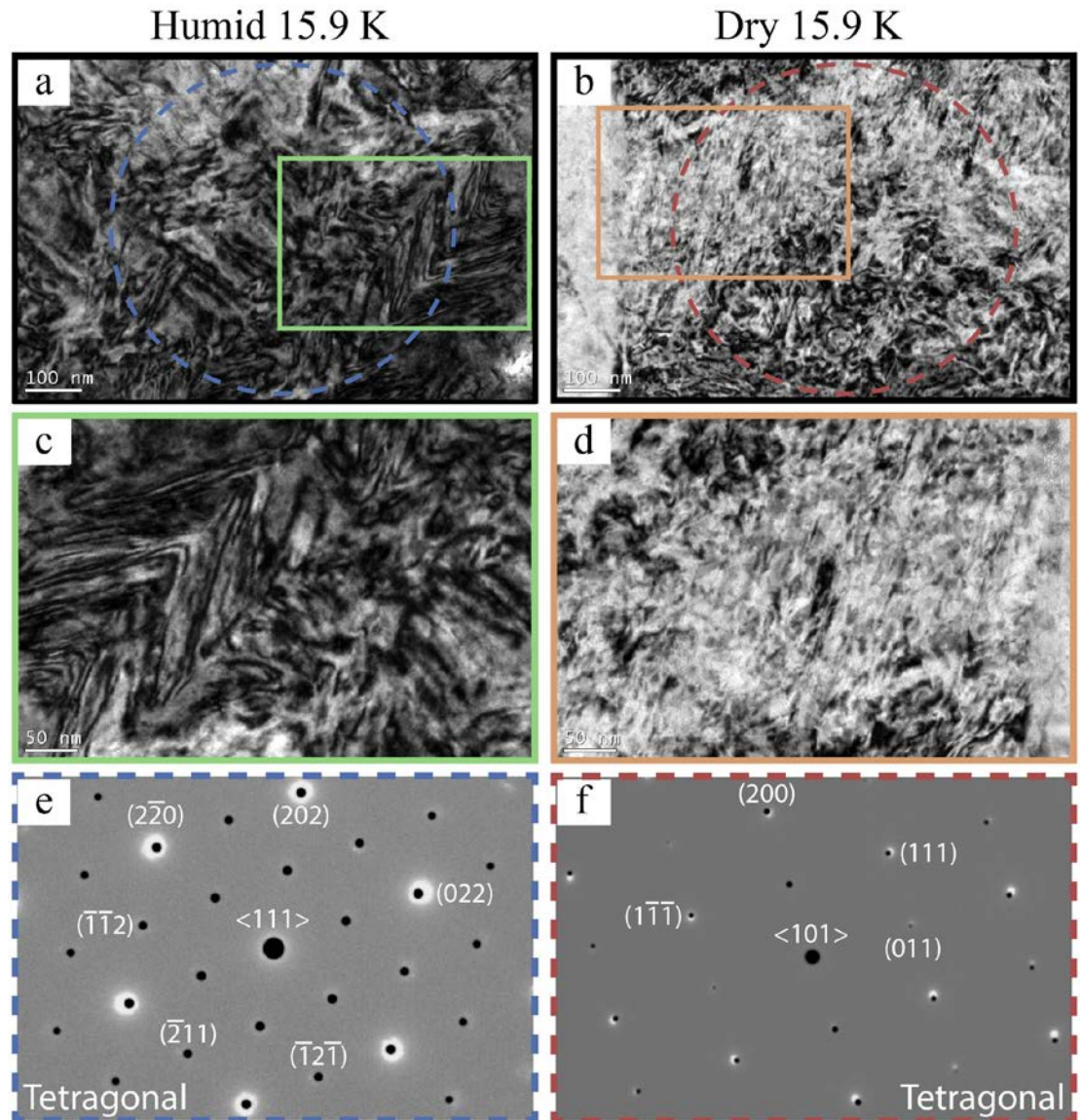
- Previous work investigated the microstructure of aged APS 8YSZ
- Dark-field images used to highlight the modulated structure
- EDX in the TEM used to determine the Y content in the domains
- SAD patterns used to determine the local phases



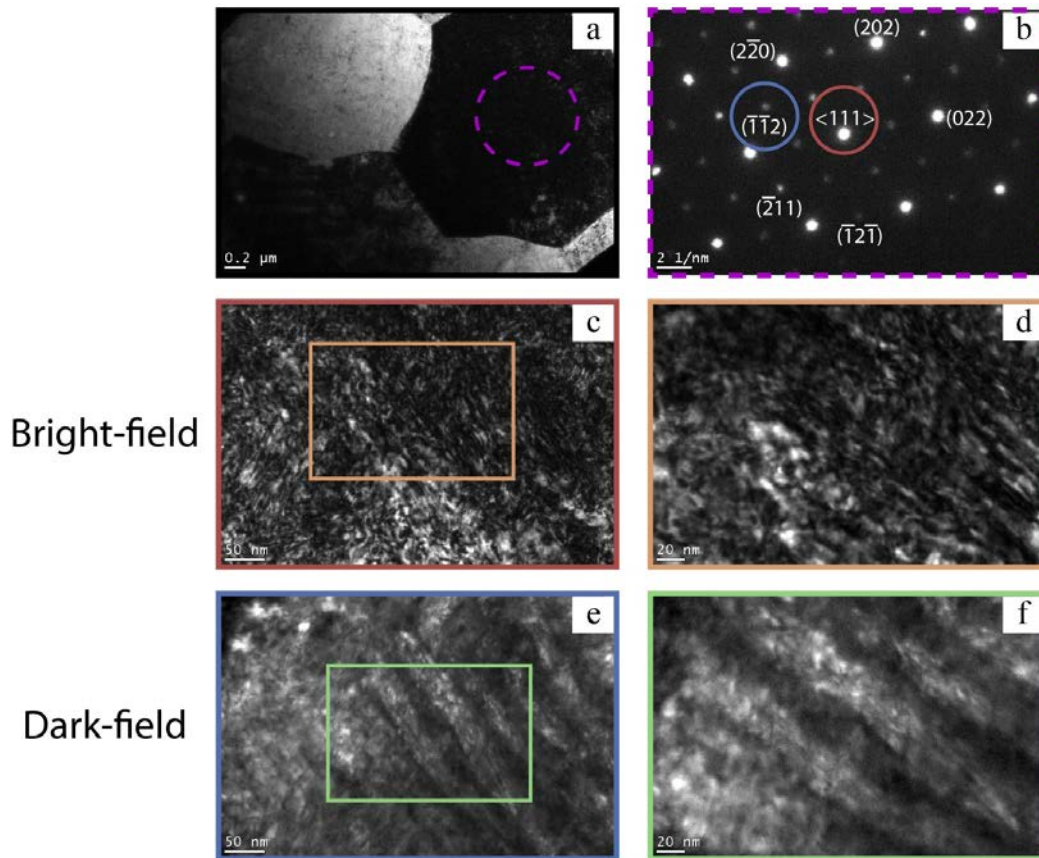
Krogstad *et al.*, *J. Am. Ceram. Soc.*, 96 [1] 299-307 (2013)

Selected Area Diffraction (SAD) of 140 hour Specimens

- Bright-field images are difficult to interpret alone
- The SAD patterns match the simulated tetragonal pattern
- The (112) reflections confirm the presence of the tetragonal phase, and are used to perform Dark Field imaging



Domain Structure Viewed Utilizing a Tetragonal Reflection



Bright-field

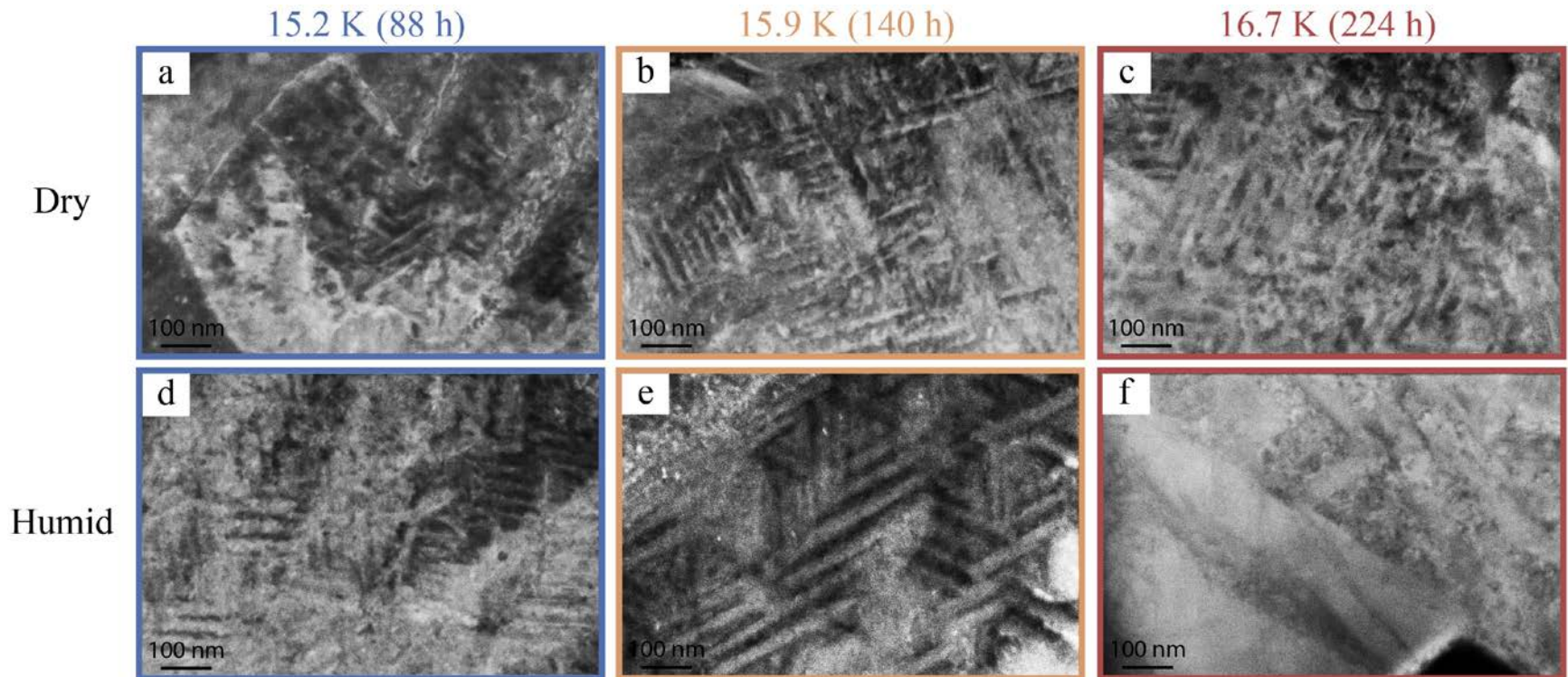
Dark-field

- TEM imaging and diffraction of the 15.9 K (140 h) humid aged sample
- Use an indexed SAD pattern to form an image from a known reflection
- Here use one of the (112) tetragonal variants to form an image
- Resulting dark-field images highlight the domains of the sample

Differences observed in domain structure:

- For dry exposures, domains exhibit ~ 3-7nm width
- For high pH₂O exposures, domains ranges from ~ 12- 17nm in width

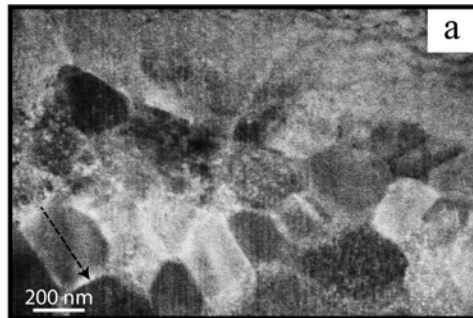
Comparison of Domain Coarsening with Aging Time



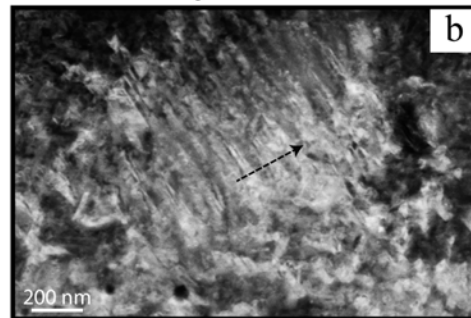
- Domains increase with increasing aging time
- At the same aging time, humid aging causes larger domains
- Larger domains are more susceptible to monoclinic transformation

Comparison of Domain Coarsening with Aging Time

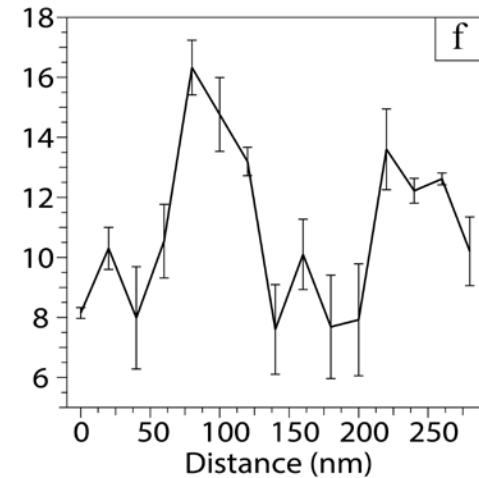
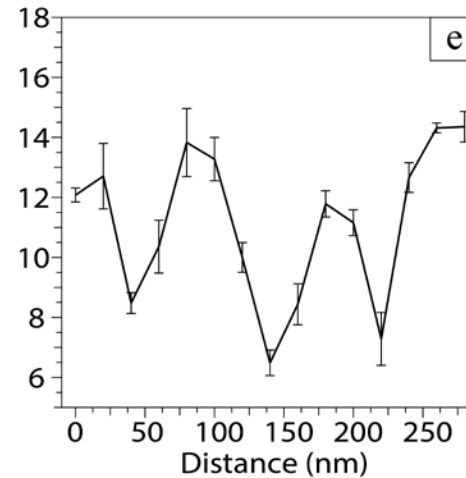
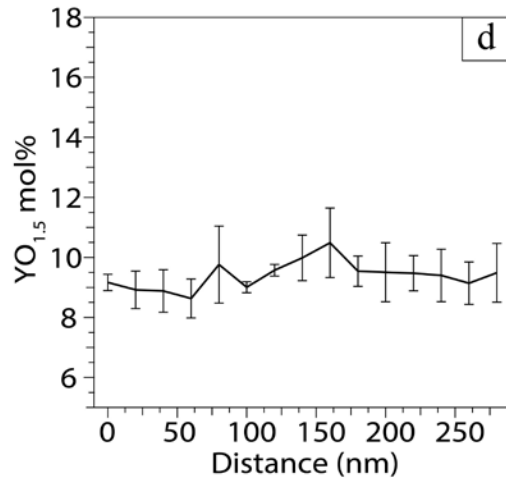
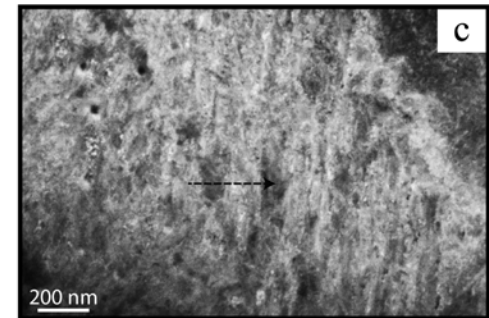
As-Received



Dry 16.7 K

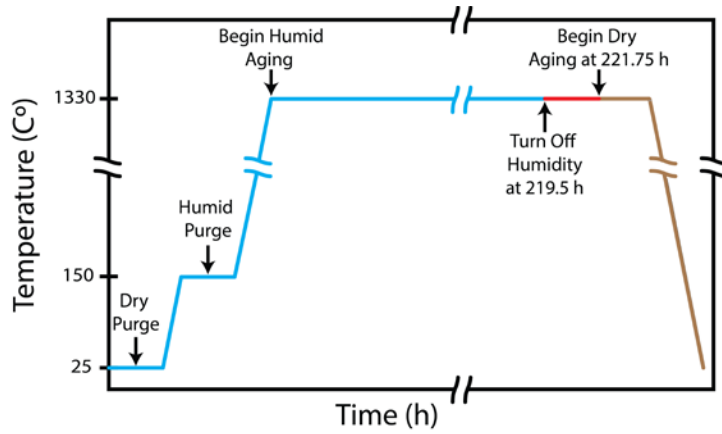


Humid 16.7 K

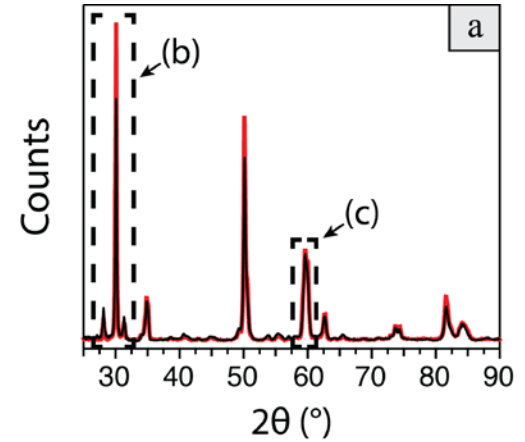


- Higher water vapor exposures show larger domain widths as measured by EDS line profiles of yttrium content

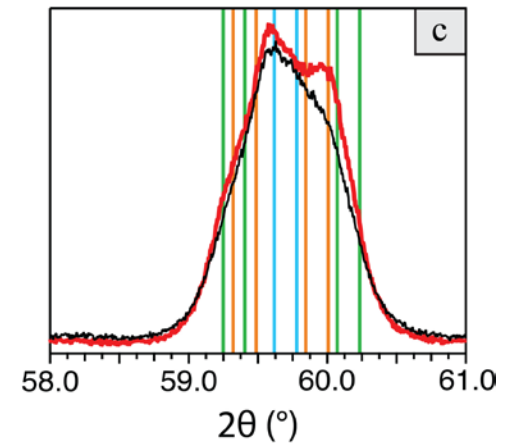
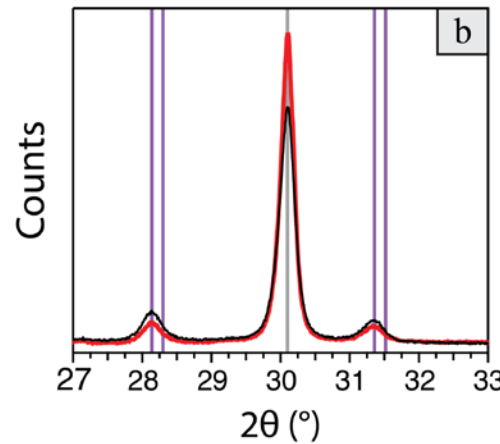
Evidence of Link Between Gas Partial Pressure and Aging



Data	
—	Dry
—	Humid
Phases	
—	t'
—	Tetragonal
—	Cubic
—	Monoclinic
—	(t') Tetragonal Cubic



Observed monoclinic formation appears to play out at high temperature, not as an artifact of low temperature exposure to high p_{H₂O} conditions.



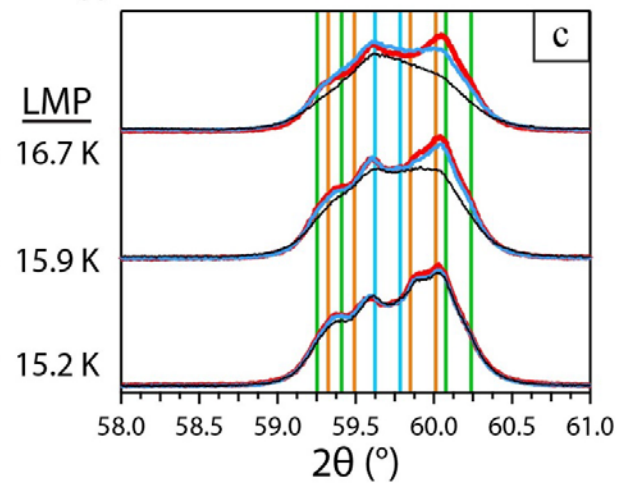
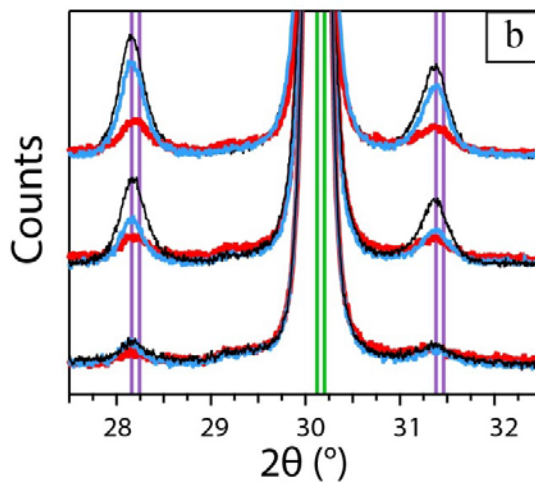
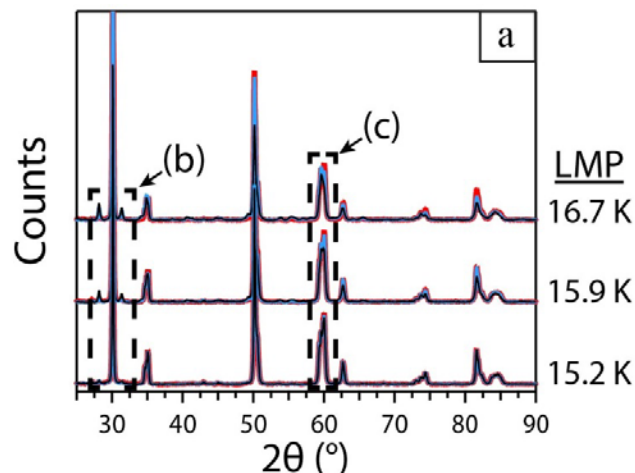
Evidence of Link Between Gas Partial Pressure and Aging

Another Variation in Exposure Environment....

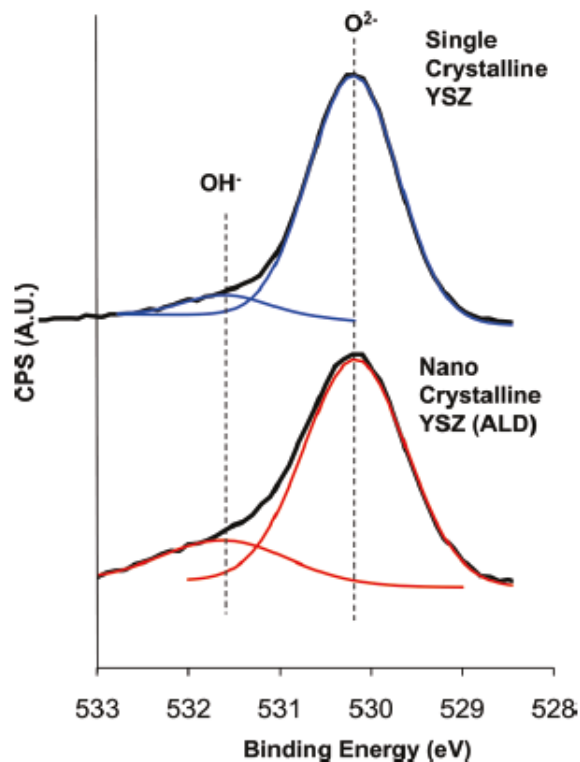
- Performed aging in a reducing environment with the same p_{H_2O}
- Purpose was to evaluate the influence of the partial pressure of oxygen.
- ✧ Utilized forming gas as the carrier gas instead of air.
- ✧ Obtained **intermediate effects** relative to Dry/Humid exposures.

Data	
—	Dry
—	Humid
—	Reducing Humid

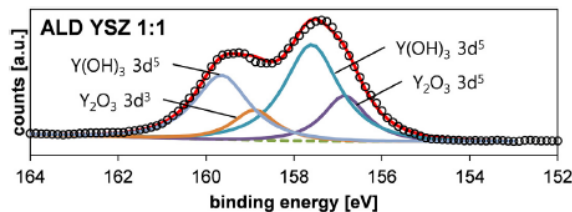
Phases	
—	t'
—	Tetragonal
—	Cubic
—	Monoclinic



XPS Analysis – Evidence of Proton Incorporation

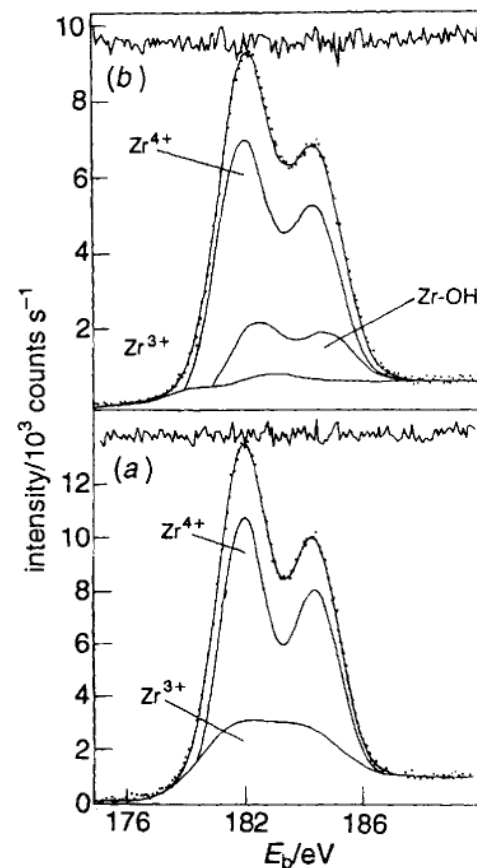


Prinz *et al.*, *Chem. Mater.*, 22 [18] 5366-5370 (1986)



Shim *et al.*, *Int. J. Hydrog. Energy.*, 39 2621-2627 (2014)

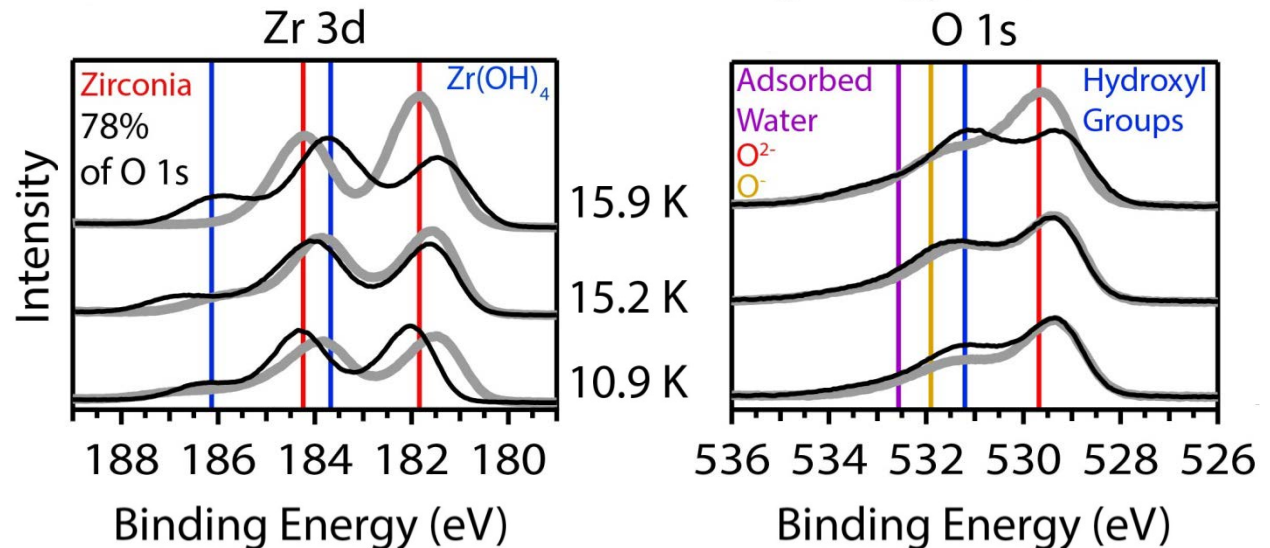
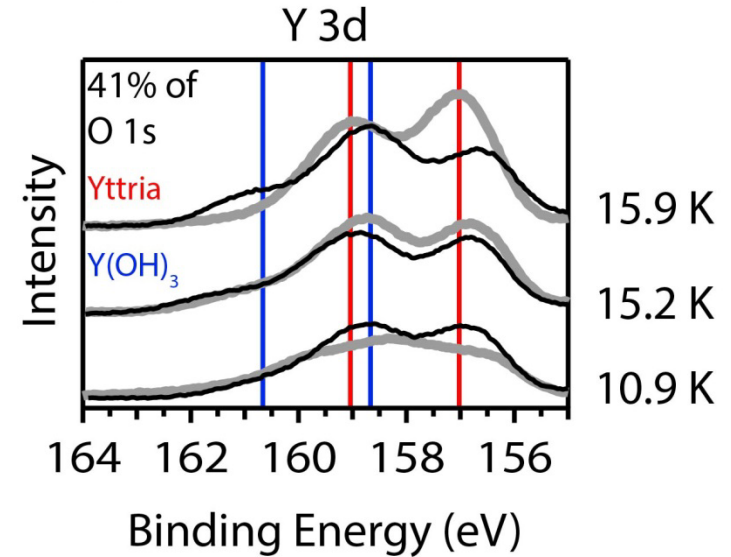
- XPS has been used to identify the formation of hydroxyl groups on YSZ.
- Can identify these groups by the increase in the binding energy due to a chemical shift.
- Can identify hydroxyl groups for various elements based on their XPS spectral lines.



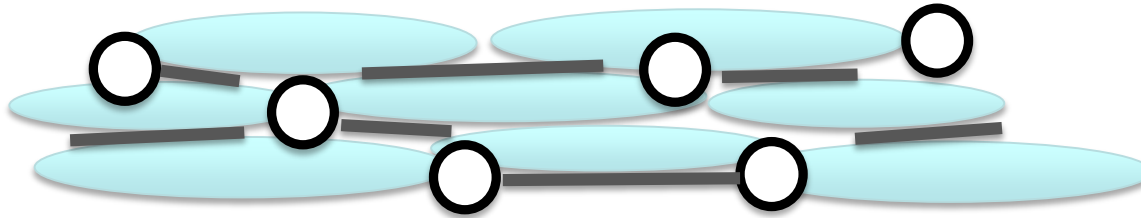
Badwal *et al.*, *J. Mater. Chem.*, 4 [2] 257-263 (1994)

XPS Analysis – Direct Evidence of Proton Incorporation

- XPS was done on the 10.9 K (6 h), 15.2 K (88 h), and 15.9 K (140 h) thermally aged samples.
- Purpose was to determine if water derived species were incorporated into the structure.
- Evidence of hydroxyl group formation for multiple elemental shells.



Thermally Sprayed Abradable Coating Samples



Ceramic Matrix Phase

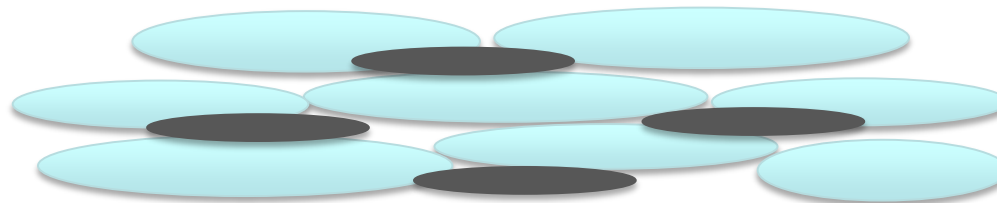
- TBC compositions
- Stabilized zirconia (Y or Dy)

Porosity

- 30-45%
- Polymer pore former (polyester)

Dislocator Phase

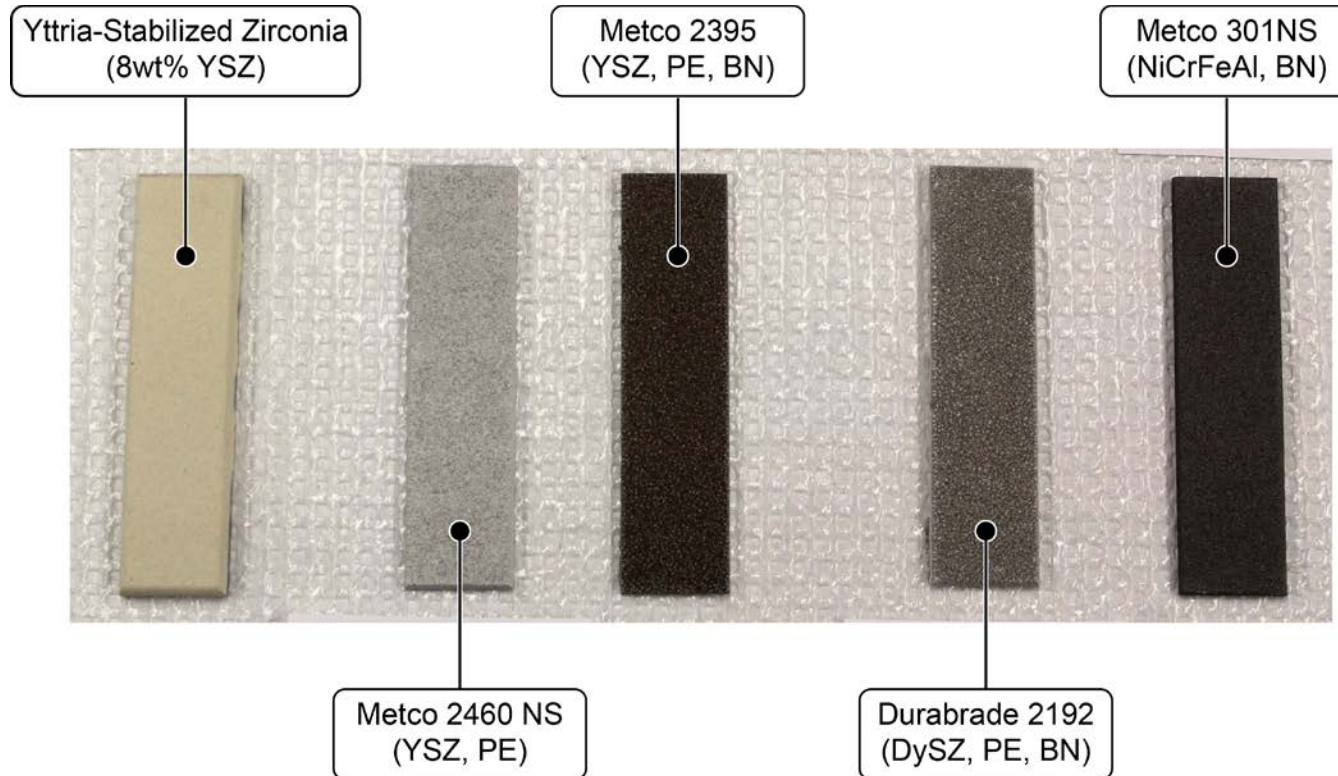
- Hexagonal boron nitride (< 1 wt. %)
- Magnesium spinel
- Lanthanum phosphate



Steinke, T. et al. Process Design and Monitoring for Plasma Sprayed Abradable Coatings. J. Thermal Spray Tech. (2014) 19, 756-64.
Ren, X. et al. Thermal Conductivity and Mechanical Properties of YSZ/LaPO₄ Composites. J. Mater. Science (2014) 49, 2243-51.

Thermally Sprayed Abradable Coating Samples

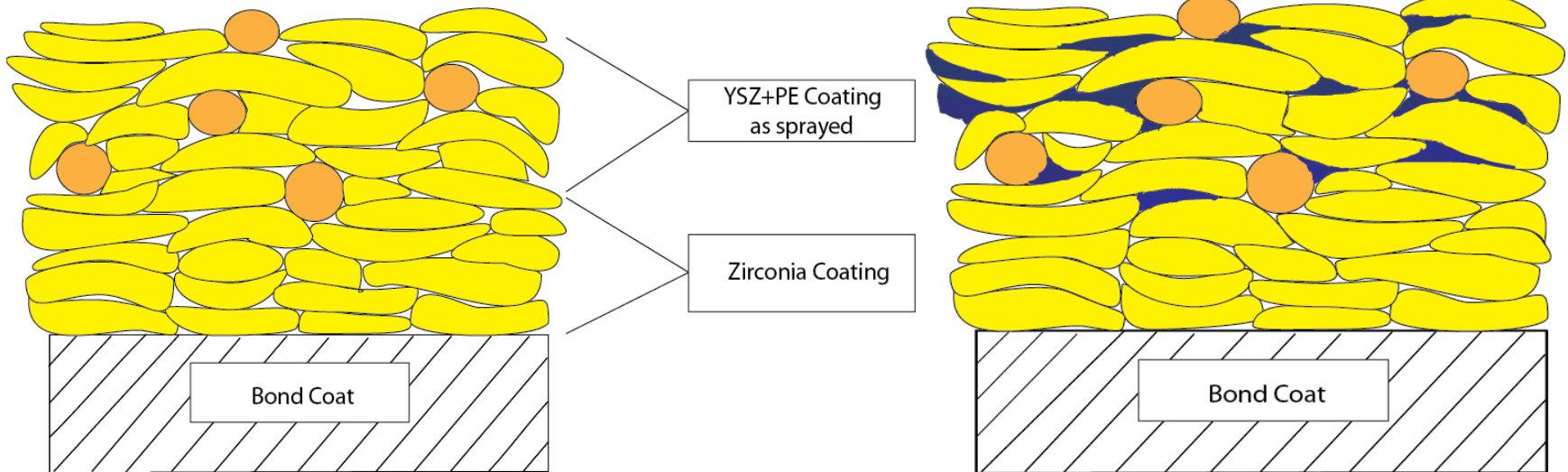
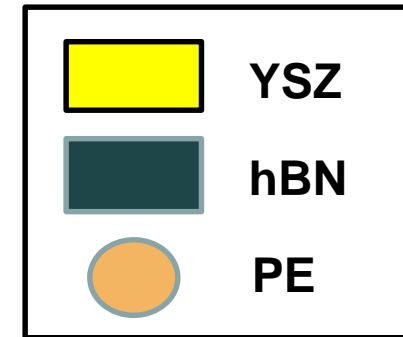
Sample coupons were prepared by Air Plasma Spraying (APS) techniques:



Solar Turbines
A Caterpillar Company

Ceramic Abradable Coating Studies

- Pure 8YSZ
- 8YSZ + PE
- 8YSZ + PE + hBN

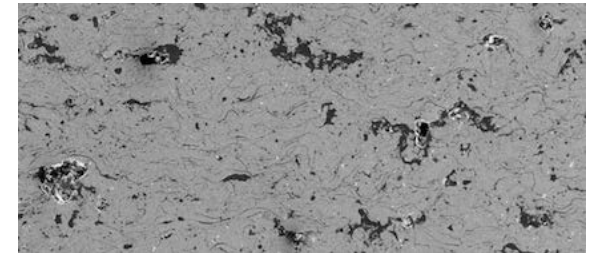


Abradable Coating System

Air plasma sprayed (APS) $9.5\text{Dy}_2\text{O}_3\text{-ZrO}_2$, hBN, polymer (DySZPB)

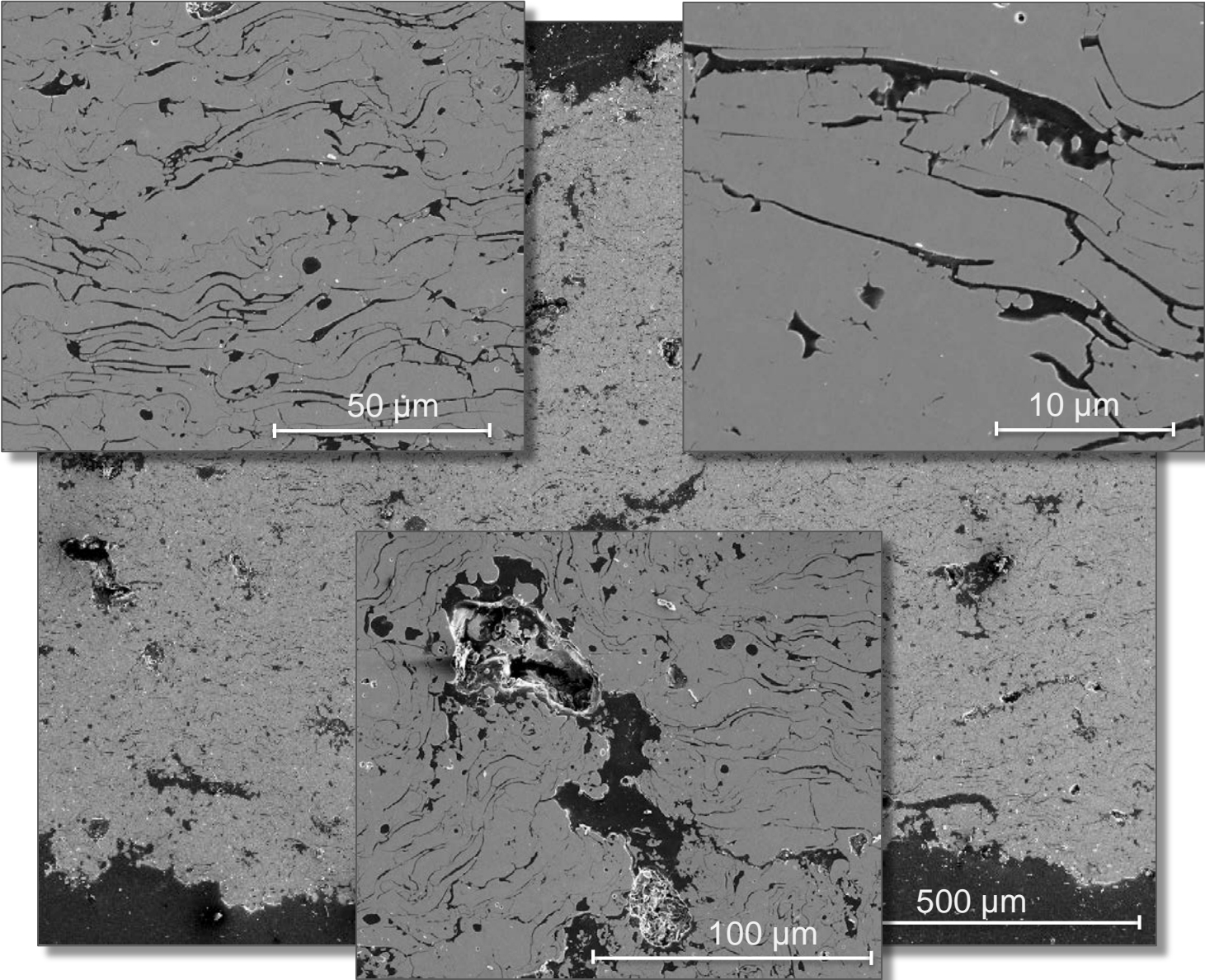
- Tetragonal DySZ provides thermal shock resistance and improved erosion resistance
- Hexagonal BN and polymer pore former increase coating abrasability

Sulzer Metco	Constituent Weight Percent (wt. %)				Operating Temp.
	ZrO ₂	Dy ₂ O ₃	hBN	Polyester	
Durabrade 2192	85.3	9.5	0.7	4.5	1200°C

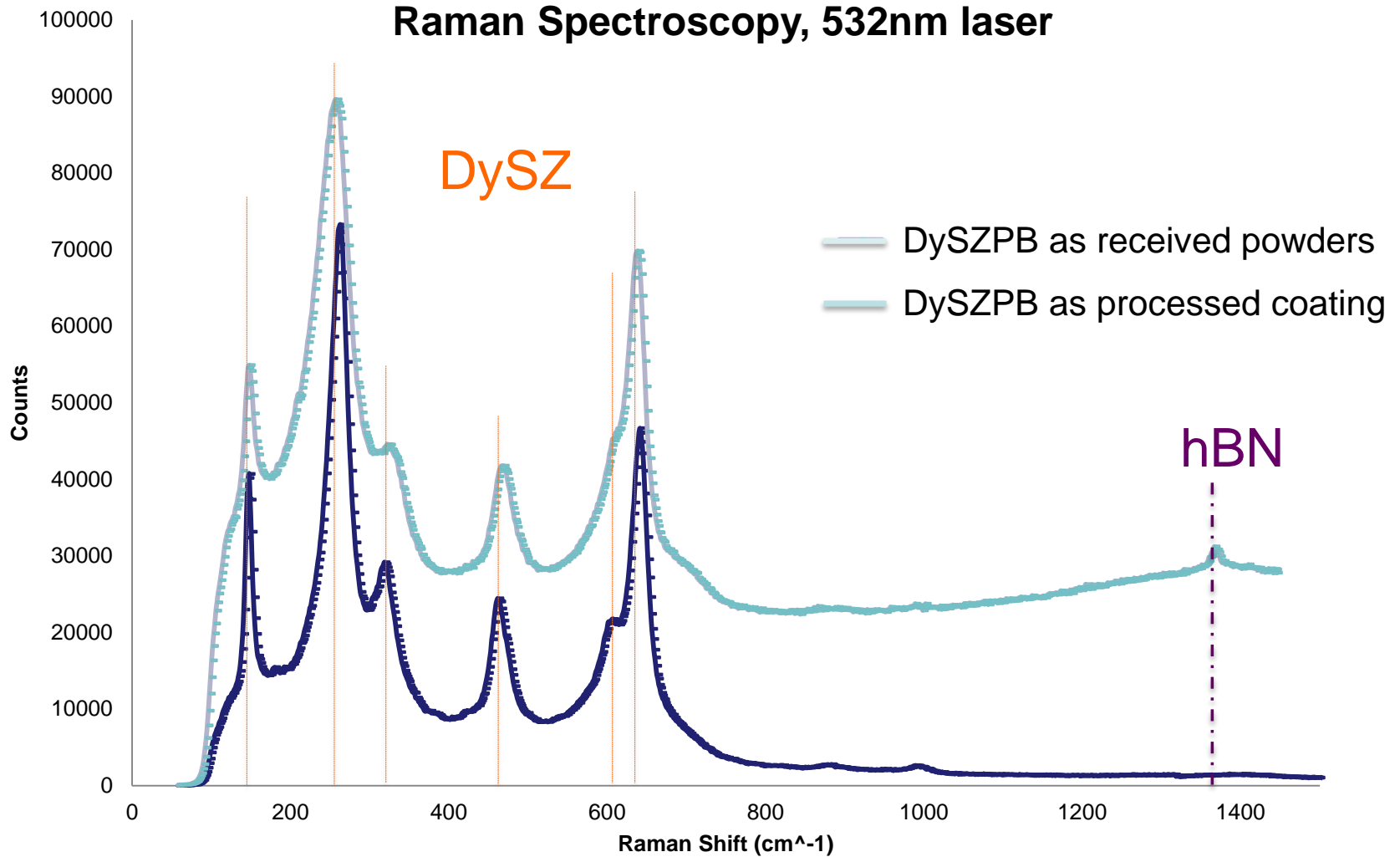


Solar Turbines
A Caterpillar Company

As-Processed Microstructure: DySZ-PE-BN



As-Processed Coating Characterization



As-Processed Coatings Incorporating BN

Amorphous B-based phase present at splat boundaries



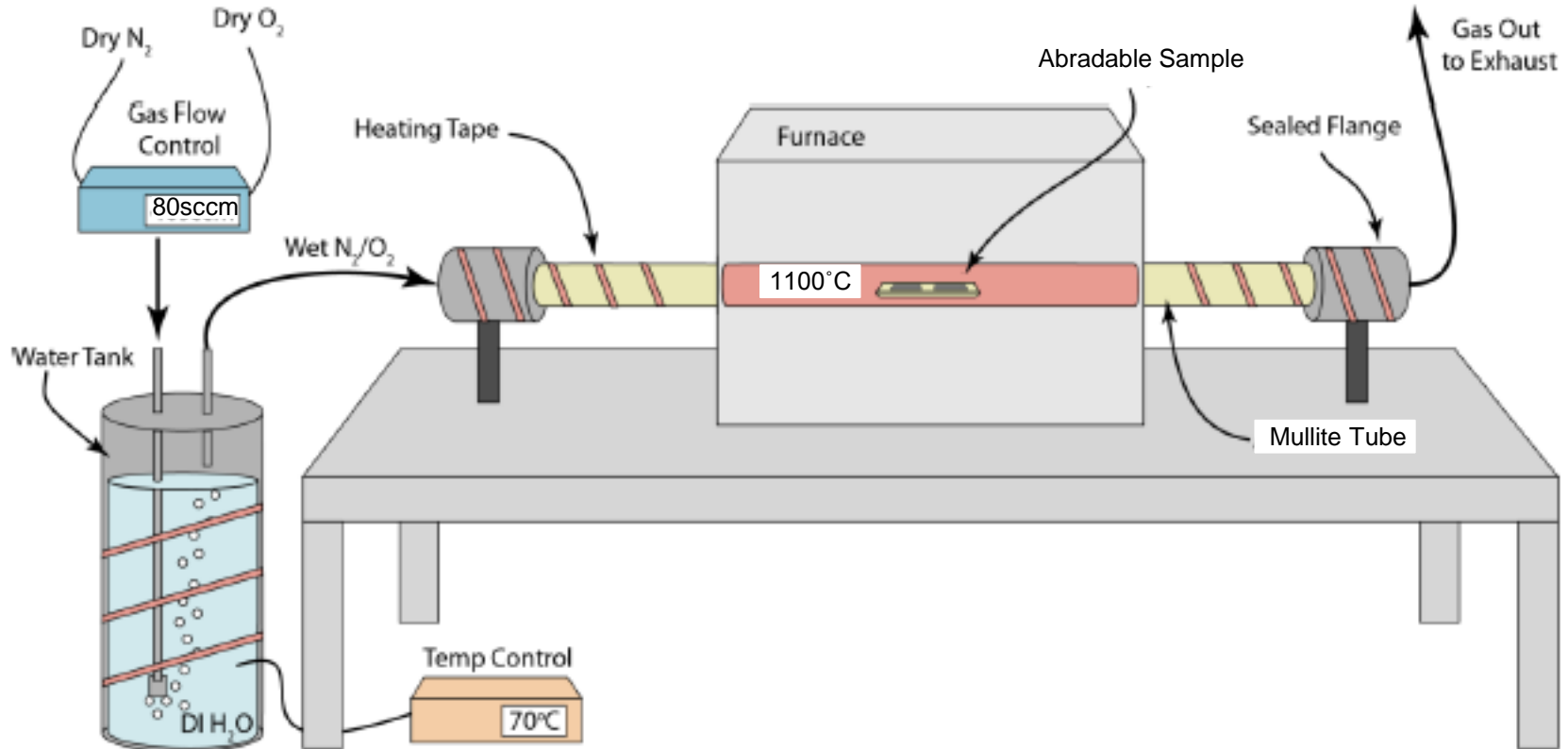
B-containing Amorphous Splat Boundary Phase

TEM imaging credit: Irvine Materials Research Institute staff, Kenta Ohtaki.

Experimental – Accelerated Degradation Studies

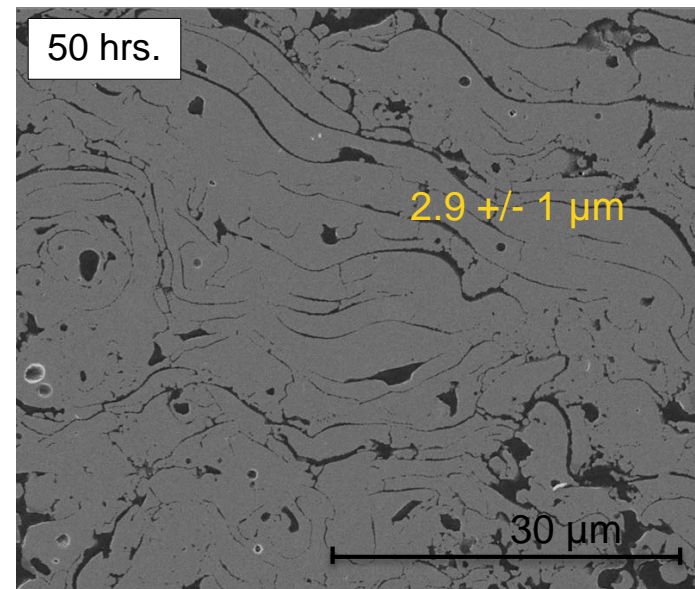
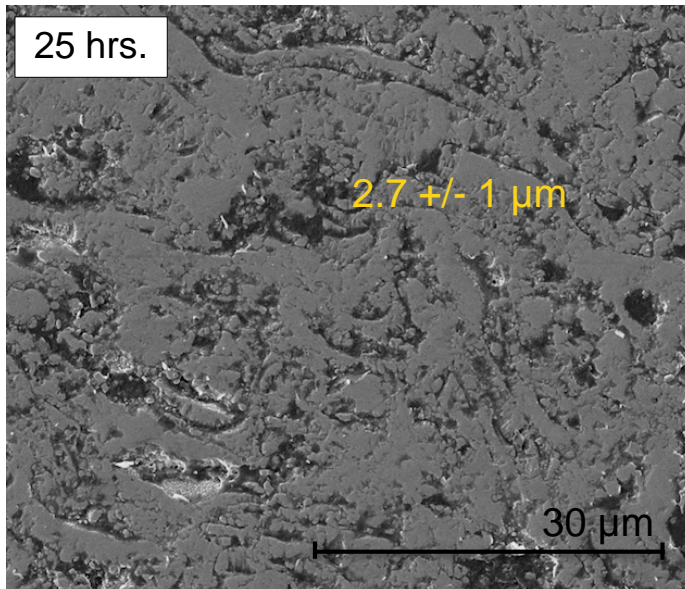
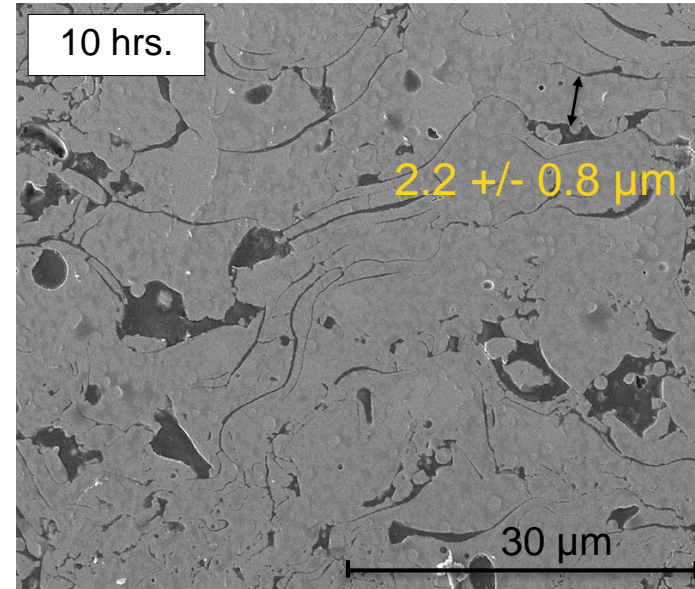
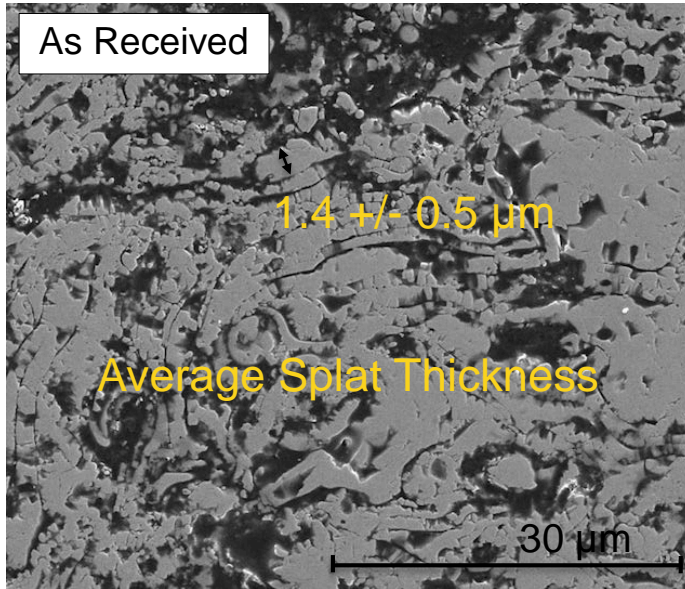
High temperature, controlled atmosphere tube furnace exposures

- Exposed at 1100°C, 10°C/min. ramp for 10, 25, 50 hrs.
- Natural gas: 9.5% H₂O (v)
- Syngas: 30% H₂O (v)

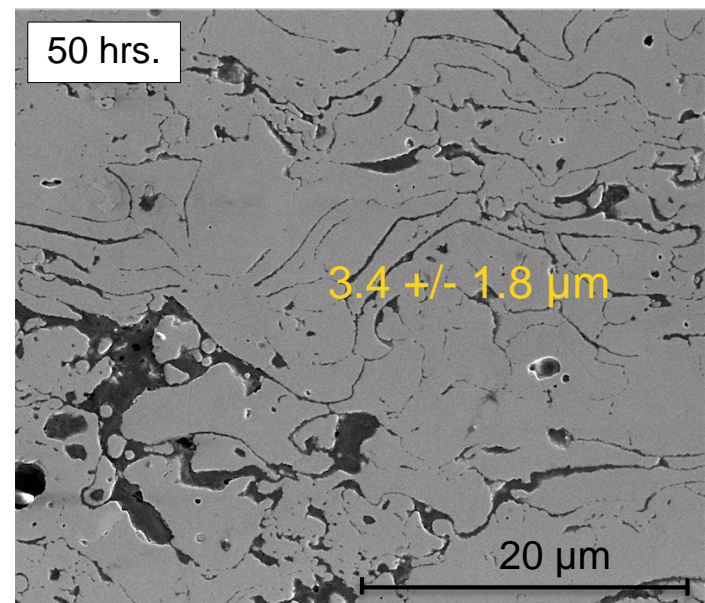
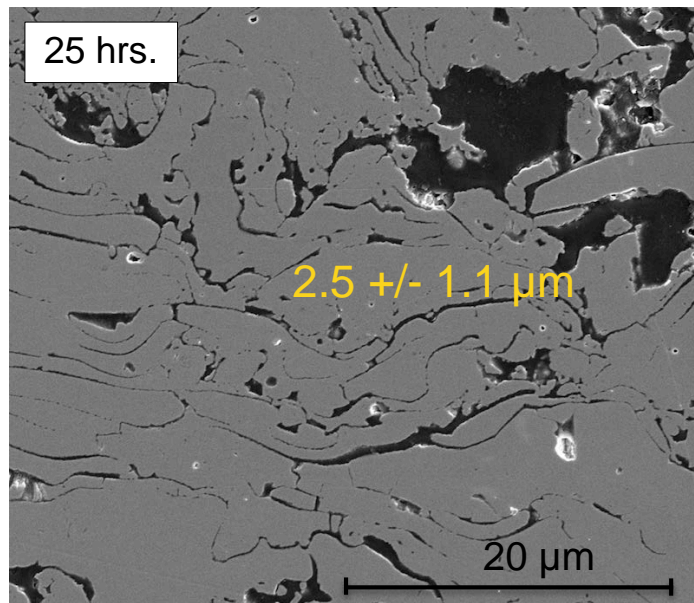
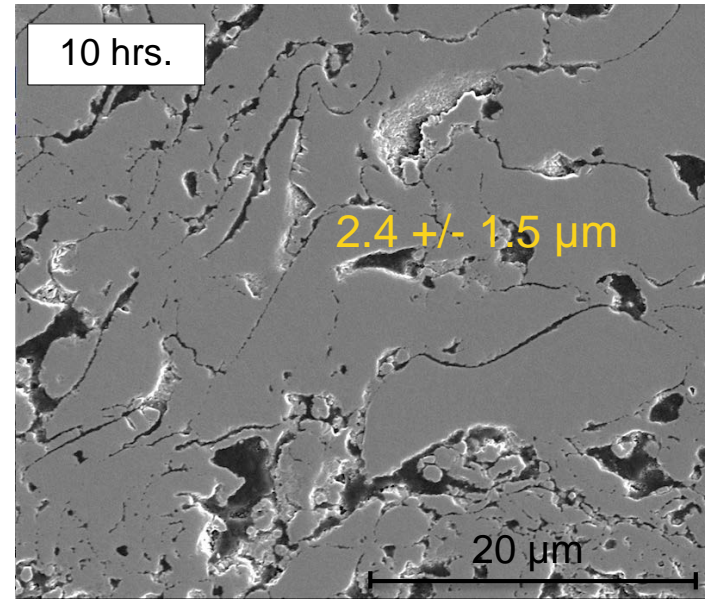
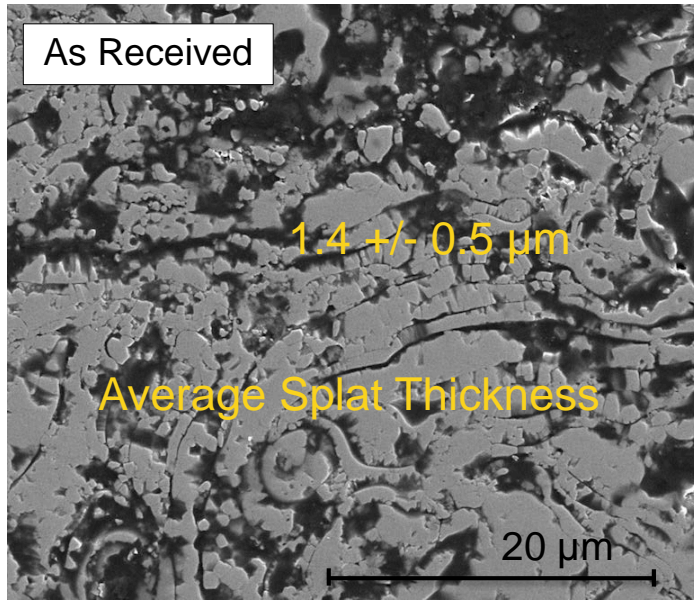


Low and High Water Vapor Environment Exposures

Exposures in 9.5% H₂O (V)



Exposures in 30% H₂O (V)

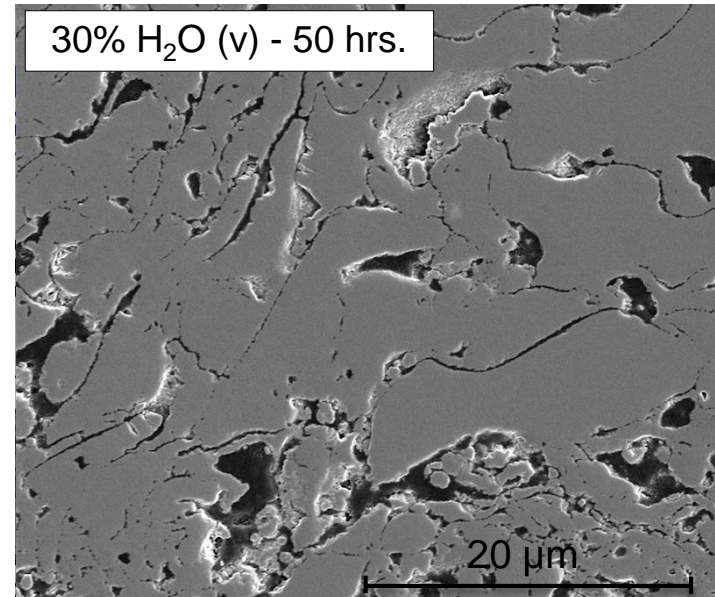
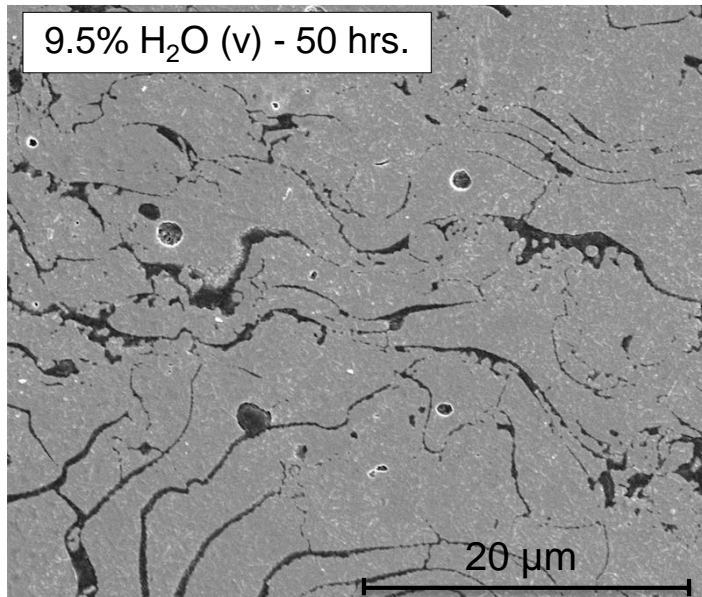
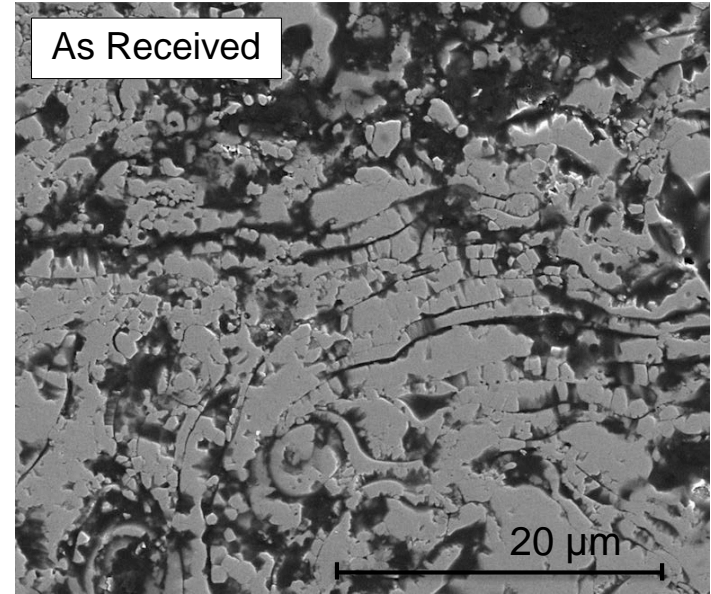


Low and High Water Vapor Exposures Compared

Compaction at surface.

Steady increase in splat size.

- 50% in low water vapor for 50 hrs.
- 60% in high water vapor for 50 hrs.



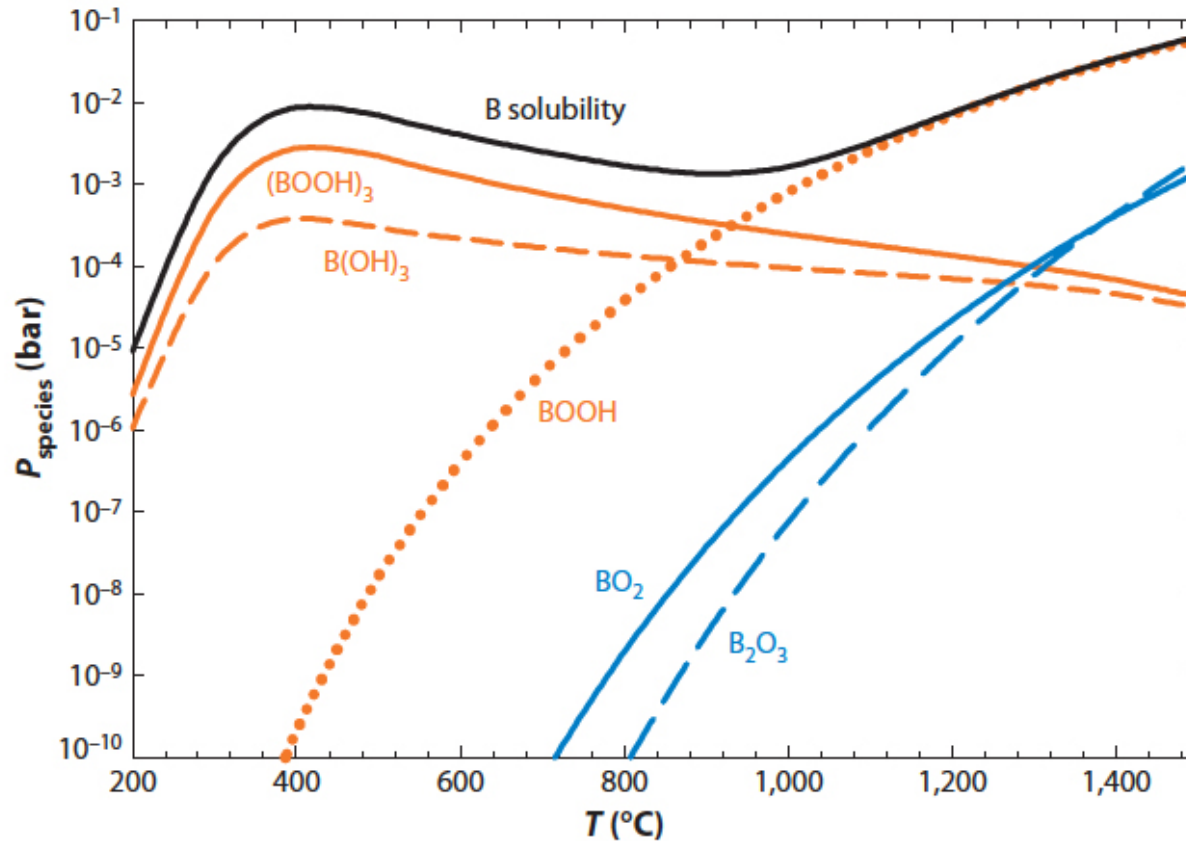
Anticipated Effects of Elevated Water Vapor on YSZ/BN

- Enhanced sintering (porosity removal)
- Tetragonal phase transformation
- Development of significant volatility in water vapor containing environments – Oxidation, volatilization of hBN



Metscher, Opila, Jacobson. Water Vapor Mediated Vaporization of High Temperature Materials (2013).
Yu, Hou. Effect of Water Vapor Content on Reaction Rate of hBN powder at 1273K.

Anticipated Effects of Elevated Water Vapor Levels

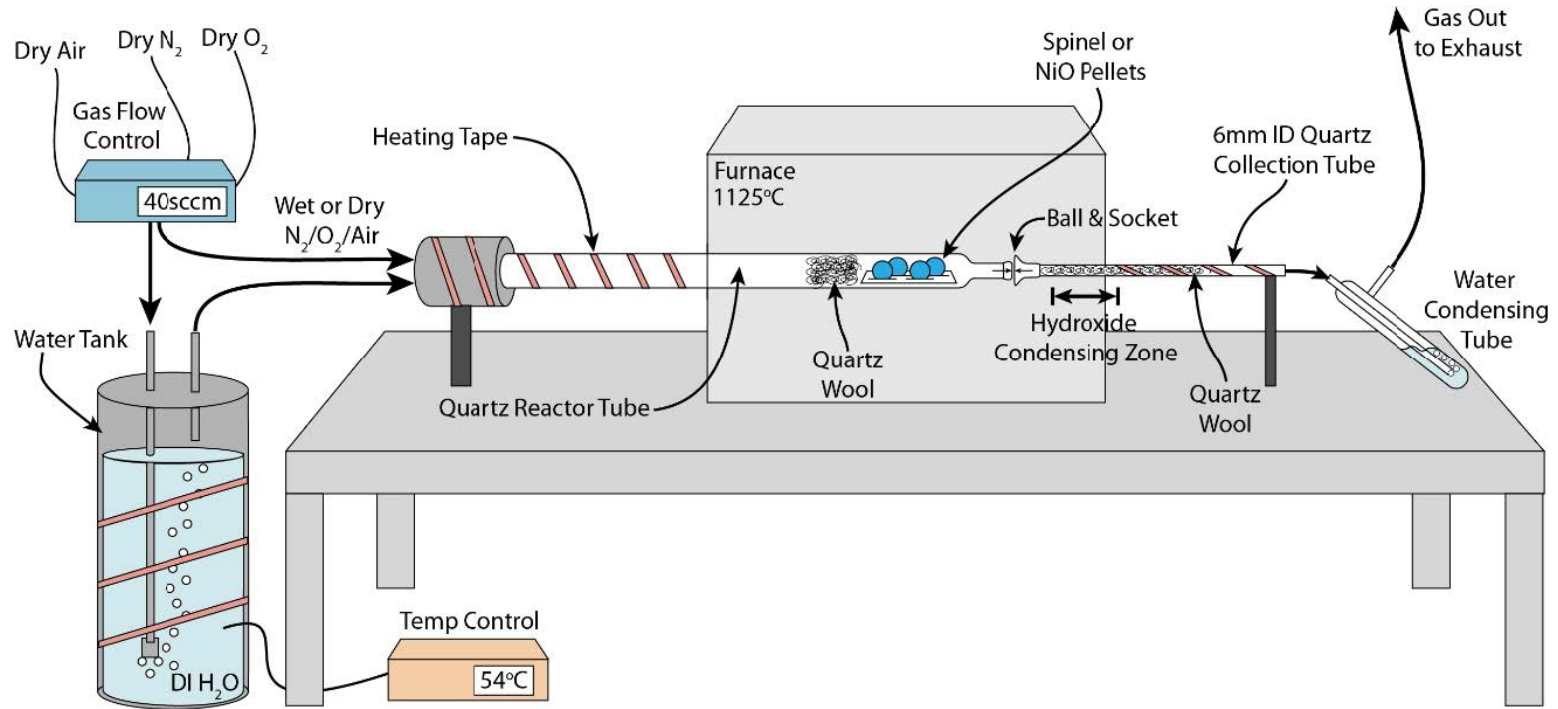


- Development of significant volatility in water vapor containing environments

P.J. Meschter, E.J. Opila and N.S. Jacobson,
Annual Review of Materials, 2013

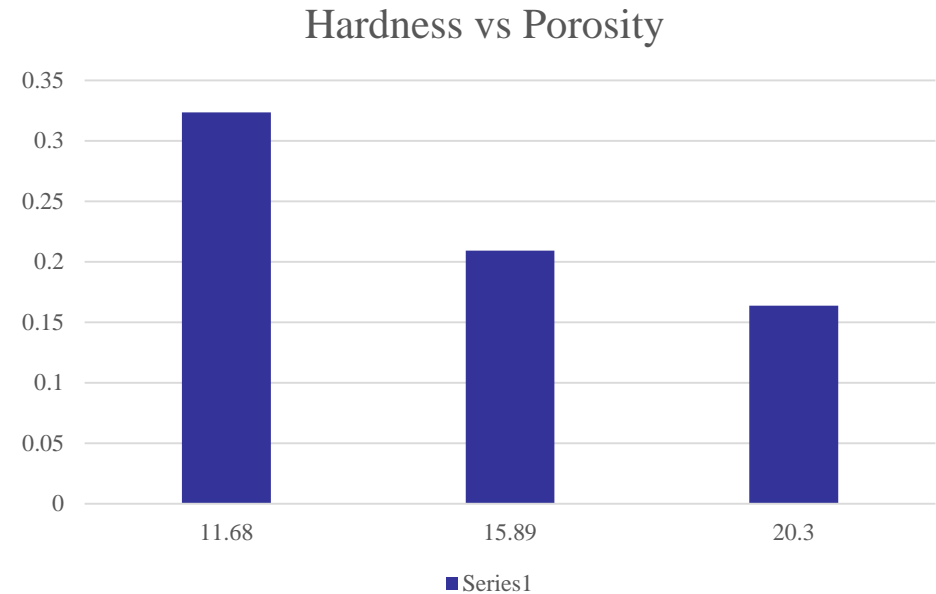
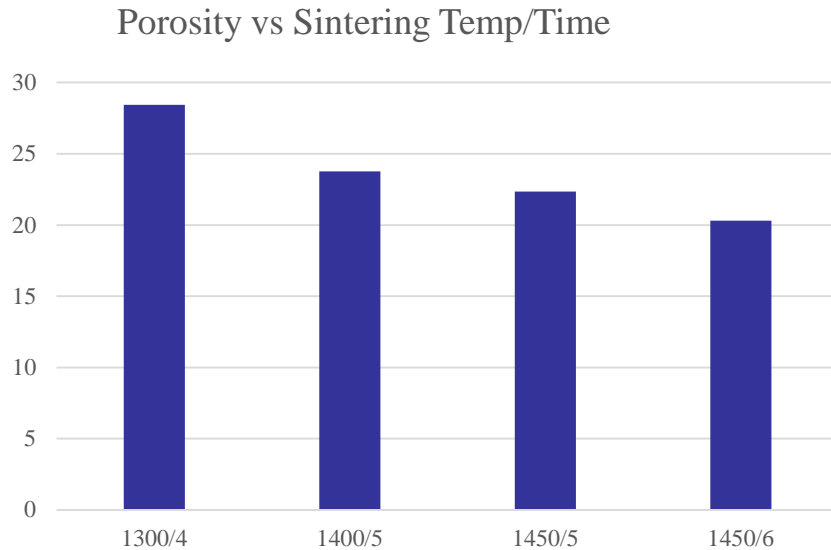
Water Vapor Effects: Volatilization of Lubricious Phases?

Transpiration experiments will be used to verify volatilization of second phase constituents (hBN species) via atomic absorption spectroscopy:

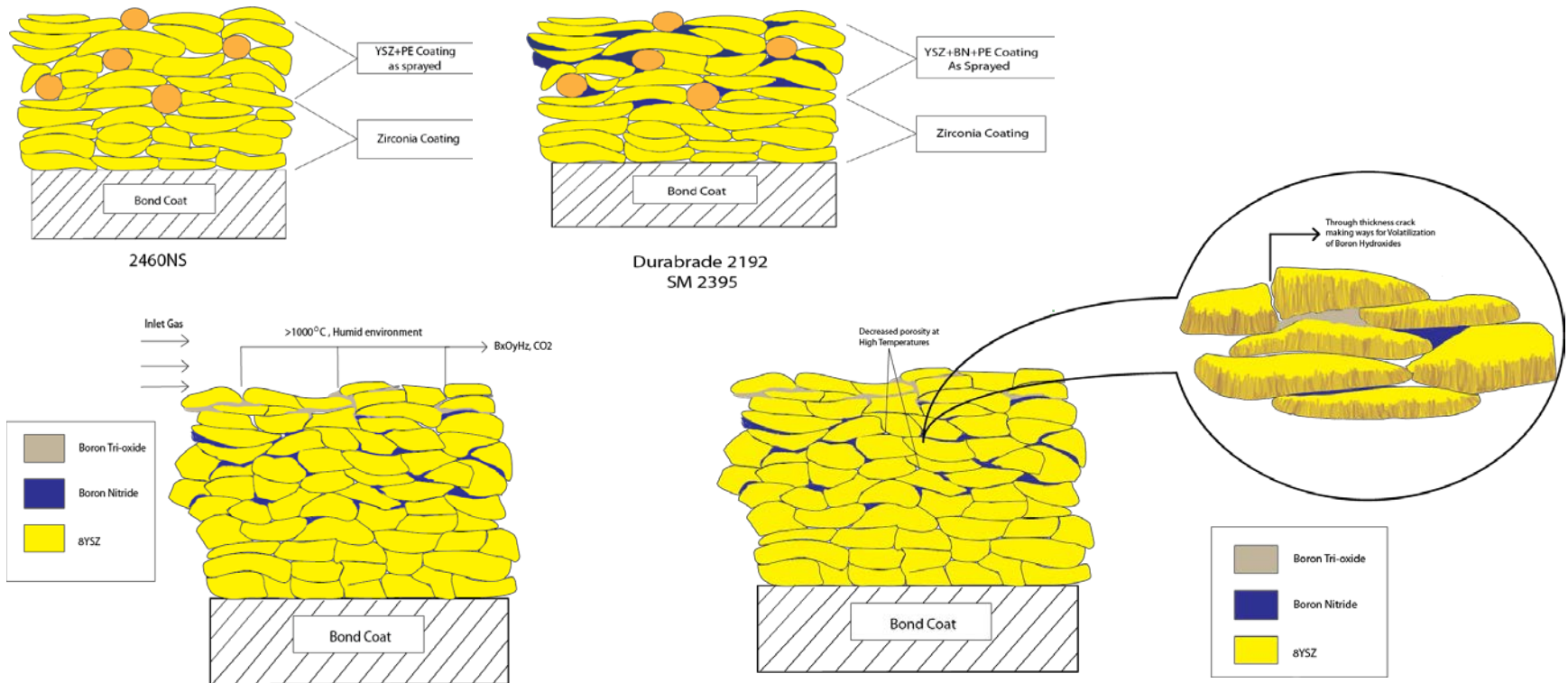


Effect of Porosity and Hardness on Exposure Conditions

- ❑ Porosity decreases with Exposure time and temperature
- ❑ Hardness increases with decrease in porosity

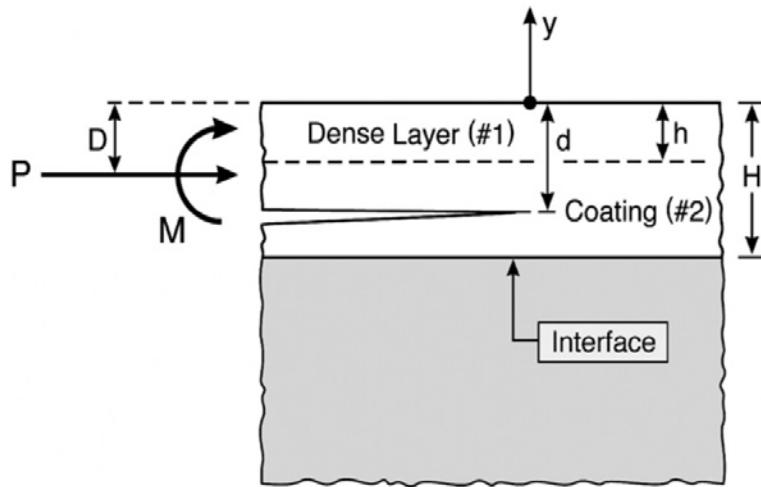


Coating Evolution – High Water Vapor Content Exposures

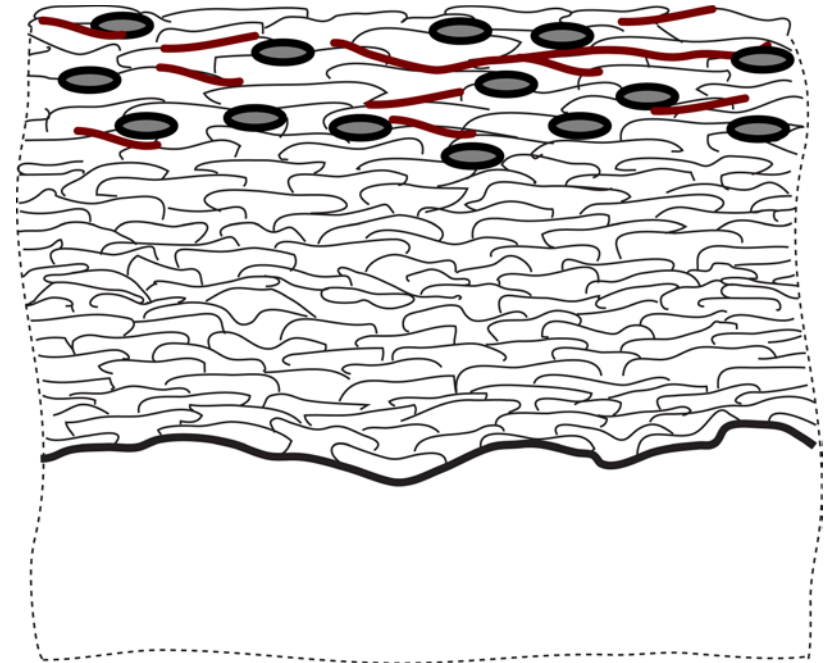


High Water Vapor Enhances Pore Sintering, and Reduces Abradability

Thermo-Mechanical Degradation



Sintering Effects

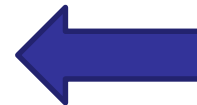
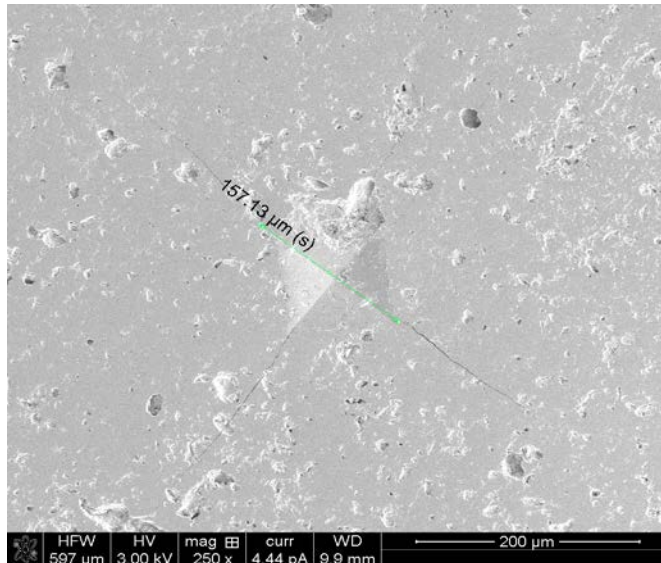
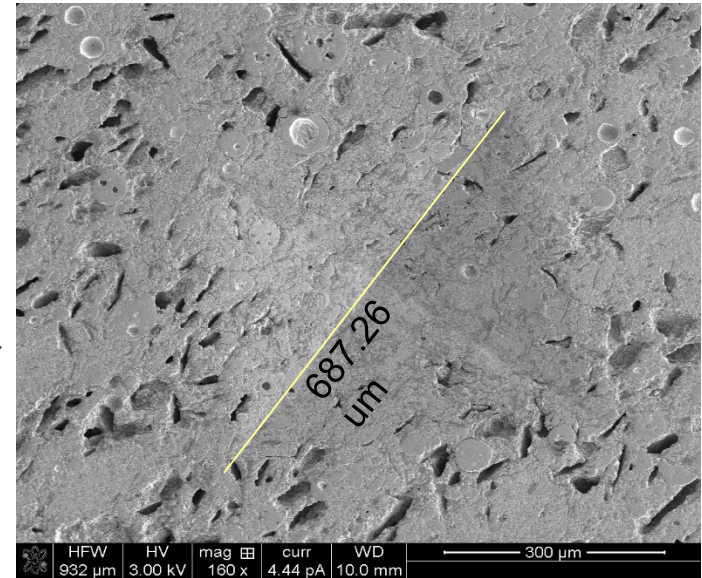


Pore Evolution,
Volatilization and
Interface Degradation

Hardness Measurements of Abradable Systems

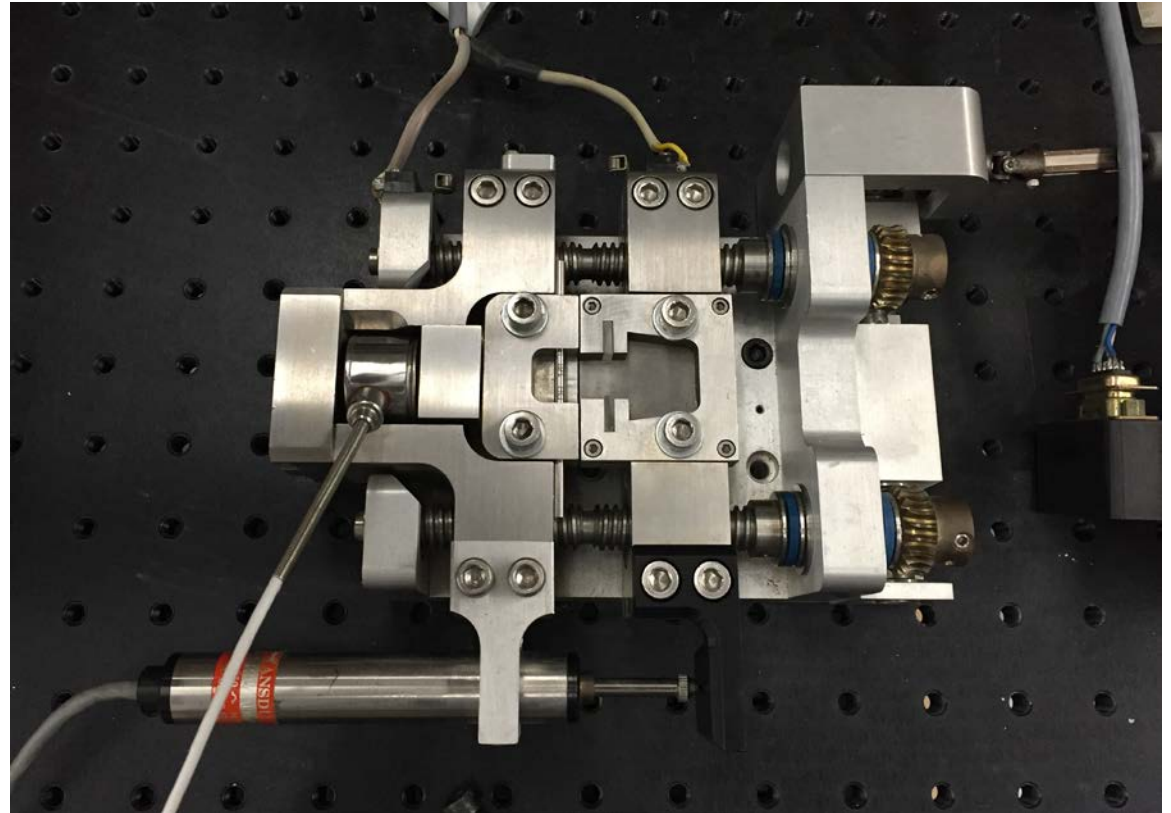
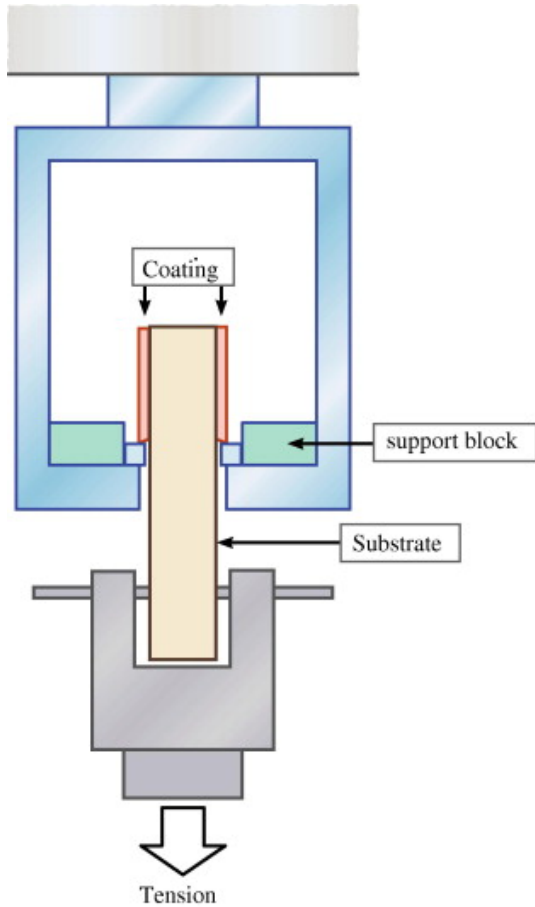
Boron Nitride acts as the lubricant phase and makes the composite more machinable and less robust.

Durabrade 2192 Indentation
~0.347 GPa
No cracks
(9 Kgf load)



Tz8Y indentation:
~7.78 GPa
Cracks visible
9 Kgf load

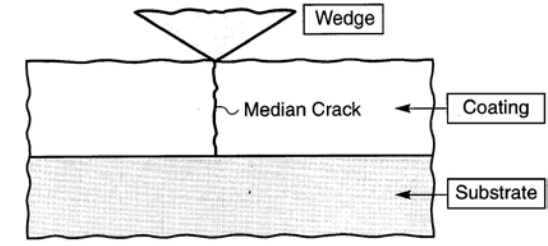
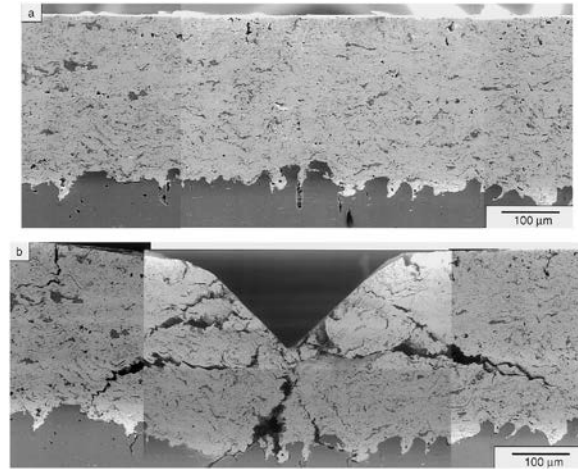
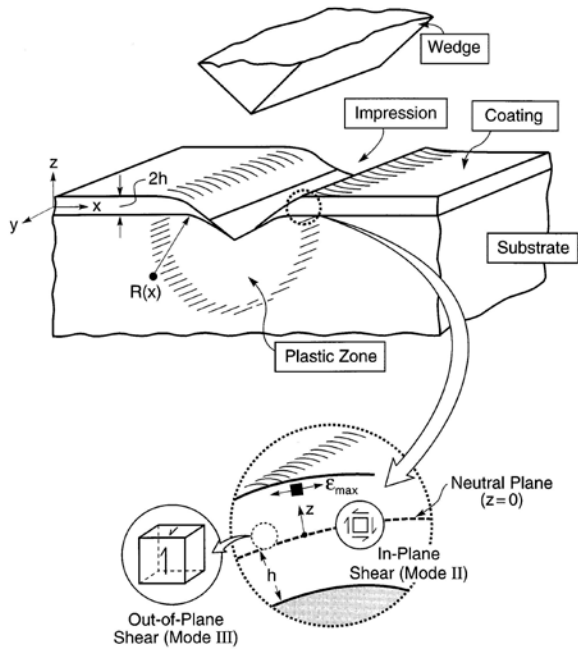
Mechanical Property Evaluations



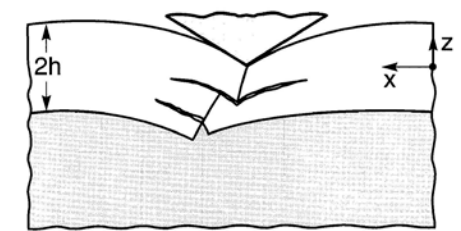
'Barb' Test System at UCI

Mechanical Property Evaluations

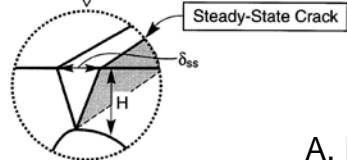
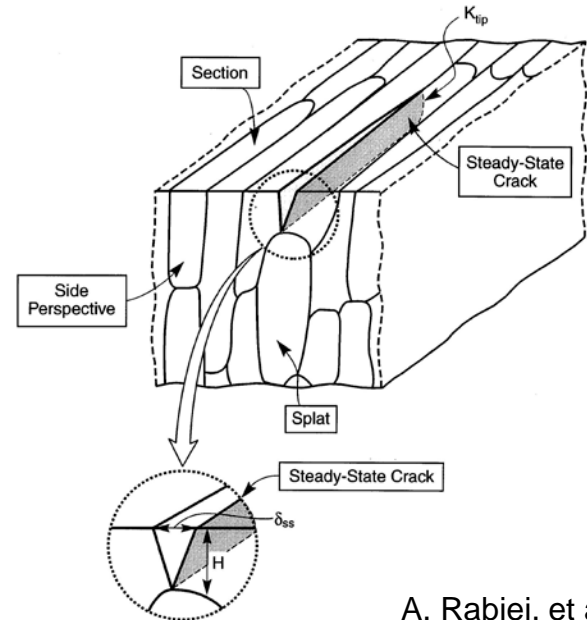
WEDGE IMPRESSION TEST



a) Median Crack



b) Bending And Lateral Cracking



Wedge Impression Test

A. Rabiei, et al, Materials Science and Engineering A, 369 (1999) 152

Abradability Test Rig

blade tip velocity:

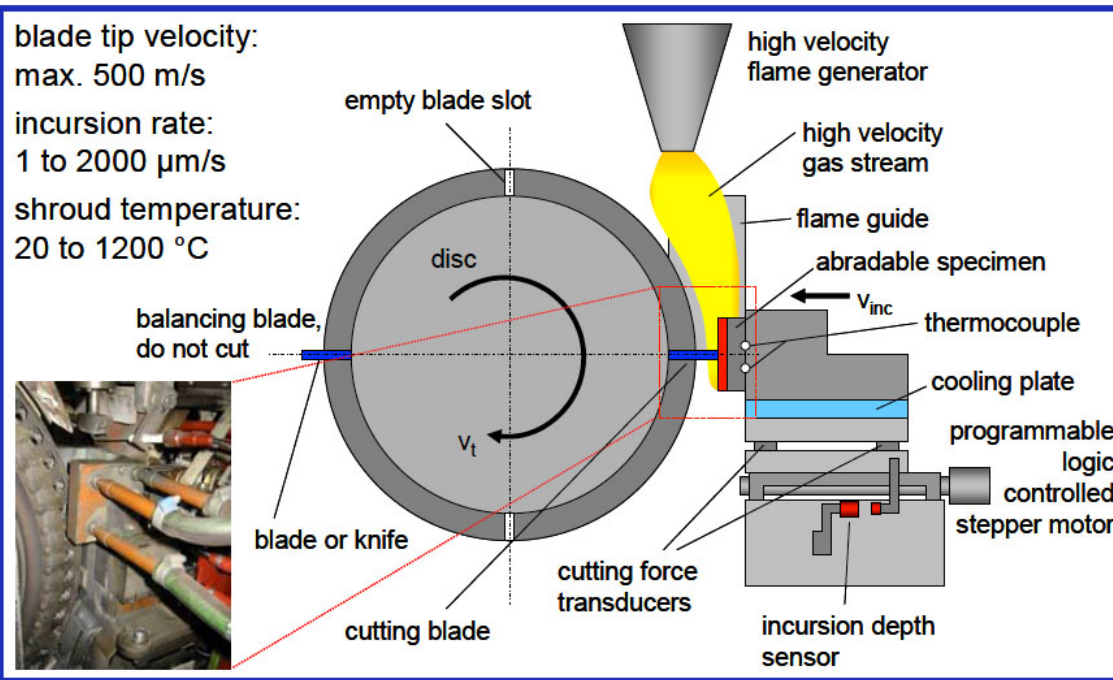
max. 500 m/s

incursion rate:

1 to 2000 $\mu\text{m/s}$

shroud temperature:

20 to 1200 $^{\circ}\text{C}$



Design features will be vetted with the OEMs and coating vendors with experience in carrying out such tests, to ensure that representative wear behavior and high temperature seal material behavior can be assessed

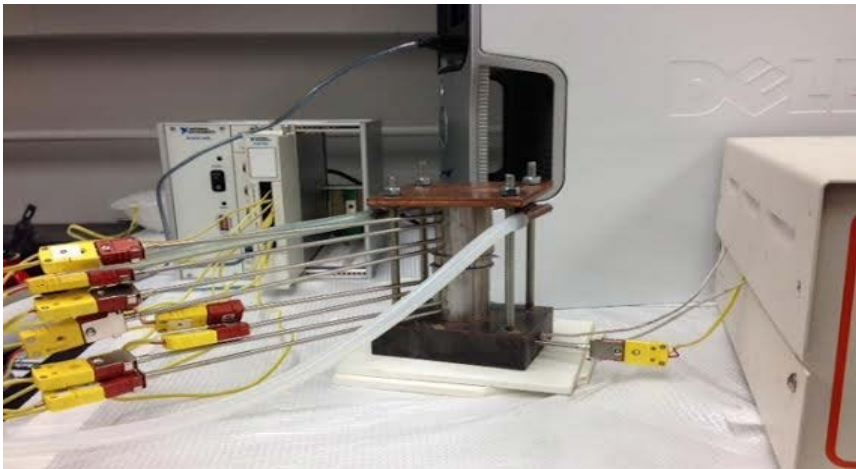
- Simulates the rubbing of blade tips against the coated casing as occurs during engine service.
- Stepper motor force the coated coupon into the moving rotor.
- Incursion rates can be accurately controlled.
- Abradability results are determined by measuring incursion depth of the blade into the coating, blade wear and abratable roughness.

D. Sporer, S. Wilson and M. Dorfman, "Ceramics for Abradable Shroud Seal Applications." *Proceedings of the 33rd International Conference on Advanced Ceramics and Composites, volume 3, 2009,*

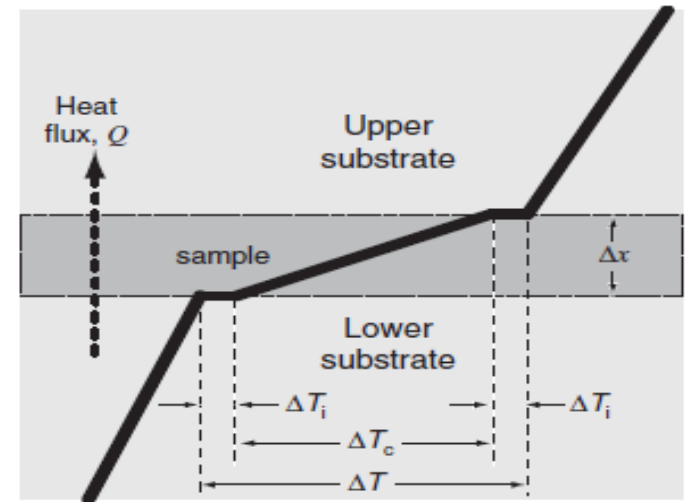
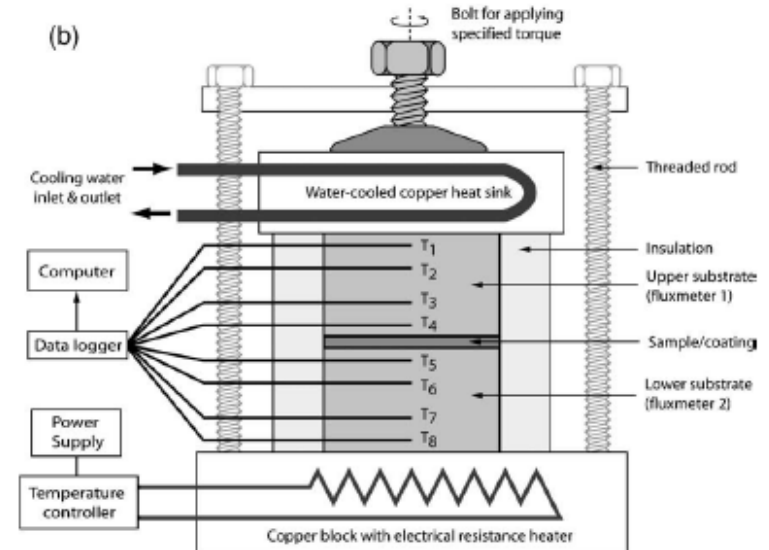
Changes to the Thermal Conductivity

- Purpose: To calculate the change in heat flow using a specimen that has been exposed to simulated water vapor environment

Current laboratory set-up



*A steady-state Bi-substrate technique for measurement of the thermal conductivity of ceramic coatings
J.C. Tan, S.A. Tsipas, I.O. Golosnoy, J.A. Curran, S. Paul, T.W. Clyne □



Summary and Key Developments and Conclusions

- YSZ aging appears accelerated in higher pH₂O environments. A strong correlation between pH₂O and *accelerated* transformation of the desired t' phase to equilibrium phases is found. XRD, Raman Spectroscopy and TEM/STEM analysis give consistent evidence of the role of high pH₂O environments on the aging/degradation process. Exposure conditions that were interrupted (“dried”) at elevated temperature provide evidence that the accelerated aging is not a low-temperature artifact.
- Degradation studies relevant to abradable coatings (hBN included) are underway. Elevated water vapor combustion environments appear to accelerate materials evolution that will lead to abradable coating loss or performance degradation.
- Mechanical and thermomechanical test approaches– for evaluation of abradable coating performance in relation to IGCC systems – are also under development
-
- **Use of IGCC combustion systems brings up additional issues in oxidation, corrosion volatilization and deposit-based degradation; the underlying mechanisms must be better understood in order to develop effective materials design strategies.**

Questions?

